Publications of the Astronomical Society of Australia (PASA), Vol. 30, e011, 23 pages.

doi:10.1017/pasa.2012.011

Absolute Magnitude Calibration for Red Giants Based on the Colour–Magnitude Diagrams of Galactic Clusters. III. Calibration with 2MASS

S. Karaali[1,2,*], S. Bilir[1] and E. Yaz Gökçe[1]

[1]Faculty of Sciences, Department of Astronomy and Space Sciences, Istanbul University, 34119 Istanbul, Turkey
[2]Email: karsa@istanbul.edu.tr

(Received June 9, 2012; Accepted August 15, 2012; Online Publication January 18, 2013)

Abstract

We present two absolute magnitude calibrations, M_J and M_{K_s}, for red giants with the colour–magnitude diagrams of five Galactic clusters with different metallicities, i.e. M92, M13, M71, M67, and NGC 6791. The combination of the absolute magnitudes of the red giant sequences with the corresponding metallicities provides calibration for absolute magnitude estimation for red giants for a given colour. The calibrations for M_J and M_{K_s} are defined in the colour intervals $1.3 \leq (V-J)_0 \leq 2.8$ and $1.75 \leq (V-K_s)_0 \leq 3.80$ mag, respectively, and they cover the metallicity interval $-2.15 \leq$ [Fe/H] $\leq +0.37$ dex. The absolute magnitude residuals obtained by the application of the procedure to another set of Galactic clusters lie in the intervals $-0.08 < \Delta M_J \leq +0.34$ and $-0.10 < \Delta M_{K_s} \leq +0.27$ mag for M_J and M_{K_s}, respectively. The means and standard deviations of the residuals are $\langle \Delta M_J \rangle = 0.137$ and $\sigma_{M_J} = 0.080$, and $\langle \Delta M_{K_s} \rangle = 0.109$ and $\sigma_{M_{K_s}} = 0.123$ mag. The derived relations are applicable to stars older than 4 Gyr, the age of the youngest calibrating cluster.

Keywords: globular clusters: individual (M13, M71, M92), open clusters and associations: individual (M67, NGC 6791), stars: distances, red giants.

1 INTRODUCTION

Systematic studies of star clusters help us to understand the Galactic structure and star formation processes as well as stellar evolution. By utilising colour–magnitude diagrams of the stars observed in the optical/near-infrared (NIR) bands, it is possible to determine the underlying properties of the clusters such as age, metallicity and distance. Colour–magnitude diagrams of star clusters can be used as a good distance indicator. The distance to a star can be evaluated by trigonometric or photometric parallaxes. Trigonometric parallaxes are only available for nearby stars where *Hipparcos* (ESA 1997) is the main supplier for the data. For stars at large distances, the use of photometric parallaxes is unavoidable. In other words, the study of the Galactic structure is strictly tied to the precise determination of absolute magnitudes.

Different methods can be used for absolute magnitude determination, where most of them are devoted to dwarfs. The method used in the Strömgren's *uvby–β* (Nissen & Schuster 1991) and in the *UBV* (Laird, Carney, & Latham 1988) photometry depends on the absolute magnitude offset from a standard main sequence. In recent years, the derivation of absolute magnitudes has been carried out by means of colour–absolute magnitude diagrams of some specific clusters whose metal abundances are generally adopted as the mean metal abundance of a Galactic population, such as thin, thick discs and halo. The studies of Phleps et al. (2000) and Chen et al. (2001) can be given as examples. A slightly different approach is that of Siegel et al. (2002), where two relations, one for stars with solar-like abundances and another for metal-poor stars, were derived between M_R and the colour index $R-I$, where M_R is the absolute magnitude in the R filter of the Johnson system. For a star of given metallicity and colour, absolute magnitude can be estimated by *linear* interpolation of *two* ridgelines and by means of *linear* extrapolation beyond the metal-poor ridgeline.

The most recent procedure used for absolute magnitude determination consists of finding the most likely values of the stellar parameters, given the measured atmospheric ones, and the time spent by a star in each region of the H–R diagram. In practice, researchers select the subset of isochrones

[*] Retired.

Table 1. Data for Five Clusters

Cluster	l (°)	b (°)	$E(B-V)$ (mag)	μ_0 (mag)	[Fe/H] (dex)	Ref.
M92	68.34	+34.86	0.025	14.72	−2.15	1
			0.020	14.59	−2.31	2
			0.023	14.55	−2.40	3
M13	59.01	+40.91	0.020	14.38	−1.41	1
			0.020	14.27	−1.53	2
			0.016	14.35	−1.60	3
M71	56.75	−4.56	0.280	12.83	−0.78	4
			0.250	13.03	−0.78	2
			0.220	13.10	−0.80	3
M67	215.70	+31.90	0.038	9.53	−0.04	1
			0.041	9.59	−0.009	5
			0.050	9.43	−0.09	6
NGC 6791	69.66	+10.90	0.150	13.10	0.37	3
			0.150	13.14	0.45	7
			0.100	12.94	0.37	8

Notes. We used the data in the first line for each cluster for absolute magnitude calibration, whereas those in the second and third lines are for comparison purposes. l and b are the Galactic longitude and latitude of the clusters; the symbol μ_0 indicates the true distance modulus of the cluster. References: (1) Gratton et al. (1997); (2) Harris (2010); (3) Brasseur et al. (2010); (4) Hodder et al. (1992); (5) Sarajedini, Dotter, & Kirkpatrick (2009); (6) Hog & Flynn (1998); (7) Anthony-Twarog, Twarog, & Mayer (2007); (8) Sandage, Lubin, & VandenBerg (2003).

with [M/H] $\pm$ $\Delta_{[M/H]}$, where $\Delta_{[M/H]}$ is the estimated error on the metallicity, for each set of derived $T_{\rm eff}$, log g and [M/H]. Then, a Gaussian weight is associated with each point of the selected isochrones, which depends on the measured atmospheric parameters and the errors considered. This criterion allows the algorithm to select only the points whose values are closed by the pipeline. For details of this procedure, we cite the works of Breddels et al. (2010) and Zwitter et al. (2010). This procedure is based on many parameters. Hence, it provides absolute magnitudes with high accuracy. Also, it can be applied to both dwarf and giant stars simultaneously.

In Karaali et al. (2003), we presented a procedure for the photometric parallax estimation of dwarf stars which depends on the absolute magnitude offset from the main sequence of the Hyades cluster. Bilir et al. (2008) obtained the absolute magnitude calibrations of the thin disc main-sequence stars in the optical M_V and in the NIR M_J bands using the recent reduced *Hipparcos* astrometric data (van Leeuwen 2007). Bilir et al. (2009) derived a new luminosity colour relation based on trigonometric parallaxes for the thin disc main-sequence stars with Sloan Digital Sky Survey (SDSS) photometry. Yaz et al. (2010) obtained transformation between optical and NIR bands for red giants. Bilir et al. (2012) extended this study to mid-infrared bands by using Radial Velocity Experiment (RAVE) Third Data Release (DR3) data (Siebert et al. 2011). Both works provide absolute magnitudes for a given photometry from another one.

In Karaali, Bilir, & Yaz Gökçe (2012a, 2012b; hereafter Paper I and Paper II, respectively), we used a procedure for the absolute magnitude estimation of red giants by using the $V_0 \times (B-V)_0$ and $g_0 \times (g-r)_0$ apparent magnitude–colour diagrams of Galactic clusters with different metallicities. Here, we extend our procedure to Two Micron All Sky Survey (2MASS; Skrutskie et al. 2006) photometry. We aim to estimate M_J and M_{K_s} absolute magnitudes for red giants with $J_0 \times (V-J)_0$ and $K_{s_0} \times (V-K_s)_0$ colour–magnitude diagrams. The outline of the paper is as follows. We present the data in Section 2. The procedure used for calibration is given in Section 3, and Section 4 is devoted to summary and discussion.

2 DATA

We calibrated two different absolute magnitudes, M_J and M_{K_s}, in terms of metallicity. Hence, we used two different sets of data. The calibration of M_J with J_0 and $(V-J)_0$ is given in Section 2.1, whereas that for M_{K_s} with K_{s_0} and $(V-K_s)_0$ is presented in Section 2.2.

2.1 Data for Calibration with J_0 and $(V-J)_0$

Five clusters with different metallicities, i.e. M92, M13, M71, M67, and NGC 6791, were selected for our program (Table 1). The V magnitudes and $V-J$ colours for the clusters M92, M13, and M71 were taken from the tables in Brasseur et al. (2010), whereas the data for the clusters NGC 6791 and M67 could be provided by different procedures as explained in the following. We used Figure 1 of Brasseur et al. (2010) and obtained a set of 30 $[M_V, (V-J)_0]$ couples for the red giant branch (RGB) of the cluster NGC 6791. Then, we transformed the M_V absolute magnitudes to V apparent magnitudes by means of the apparent distance modulus of the cluster, i.e. $\mu = 13.25$ mag. Finally, we de-reddened the V magnitudes and combined them with the true colour indices $(V-J)_0$ and obtained J_0 magnitudes. The J_0 magnitudes and $(V-J)_0$ colours are not available for the cluster M67

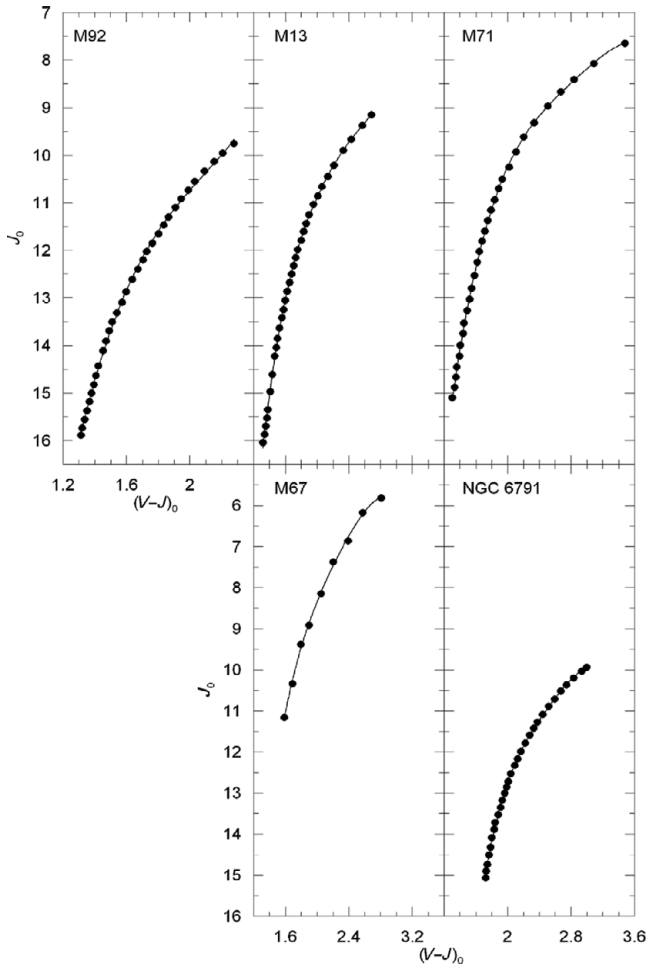

Figure 1. $J_0 \times (V-J)_0$ colour–apparent magnitude diagrams for five Galactic clusters used for the absolute magnitude calibration.

in the literature. Hence, we transformed the V, $B-V$ and $V-I$ data in Montgomery, Marschall, & Janes (1993) to obtain a set of (J_0, $(V-J)_0$) data for the RGB of M67. It turned out that 21 of the stars in the bright stars catalogue in Montgomery et al. (1993) were red giants. We de-reddened the V, $B-V$, and $V-I$ data of these stars and transformed them to $(V-J)_0$ colours by using the following equation of Yaz et al. (2010):

$$(V-J)_0 = 1.080(B-V)_0 + 0.379(V-I)_0 - 0.082[\mathrm{Fe/H}] + 0.279. \quad (1)$$

Then, we combined them with the V_0 magnitudes and obtained the J_0 ones.

We adopted $R = A_V/E(B-V) = 3.1$ to convert the colour excess to the extinction. Although different numerical values appeared in the literature for specific regions of our Galaxy, a single value is applicable everywhere. Then, we used the equations $E(V-I)/E(B-V) = 1.25$ and $E(V-J)/E(B-V) = 2.25$ of Fiorucci & Munari (2003) and McCall (2004), respectively, to evaluate the colour excesses in $V-I$ and $V-J$ colours. The intrinsic colours were evaluated by the equations $(V-I)_0 = (V-I) - E(V-I)$ and $(B-V)_0 = (B-V) - E(B-V)$.

We adopted different equations, i.e. $R = A_V/E(B-V) = 4.0$ (Turner 2012) and $E(V-J)/E(B-V) = 2.30$ (Smith 1987), and evaluated the corresponding $E(V-J)$ selective and $A_J = 1.70E(B-V)$ total absorptions for the clusters [we do not give the calculations here, only we remind to the reader that $E(V-J)$ is equivalent to $A_V - A_J$]. The results are given in Table 2. The differences between the $E(V-J)$ colour excesses estimated in our study and the ones in this paragraph are rather small. The same case holds for the A_J total absorptions except those for M71 and NGC 6791, i.e. $\Delta A_J \sim 0.2$ and 0.1, respectively, whose $E(B-V)$ colour excesses are slightly larger. We should add that the extinction equation of Turner (2012) was derived for low Galactic latitudes, i.e. the Carina region ($b \sim 0^\circ$). Whereas the Galactic latitudes of the clusters used in our study are (absolutely) greater than $b = 4^\circ\!.5$ (see Table 1). Hence, the extinction ratio and the colour excess ratios used in our study are preferable.

The range of the metallicity of the clusters in iron abundance is $-2.15 \leq [\mathrm{Fe/H}] \leq +0.37$ dex. The μ_0 true distance modulus, $E(B-V)$ colour excess, and [Fe/H] iron abundance for M92, M13, M71, and M67 were taken from Paper I, whereas those for the cluster NGC 6791 are taken from Brasseur et al. (2010), except the metallicity which is adopted

Table 2. Comparison of the Selective and Total Absorptions Evaluated by Using Different Extinction and Colour Excess Ratios

(1) Cluster	(2) $E(B-V)$	(3) $E(V-J)_p$	(4) $E(V-J)_c$	(5) $\Delta E(V-J)$	(6) $(A_J)_p$	(7) $(A_J)_c$	(8) ΔA_J
M92	0.025	0.056	0.058	0.002	0.022	0.043	0.021
M13	0.020	0.045	0.046	0.001	0.017	0.034	0.017
M71	0.280	0.630	0.644	0.014	0.244	0.476	0.232
M67	0.038	0.086	0.087	0.001	0.033	0.065	0.032
NGC 6791	0.150	0.338	0.345	0.007	0.131	0.255	0.125

Notes. Description of columns: (1) the cluster; (2) adopted $E(B-V)$ colour excess; (3) $E(V-J)_p$, the colour excess evaluated by the equation $E(V-J)/E(B-V) = 2.25$ and used in the paper; (4) $E(V-J)_c$, the colour excess evaluated by the equation $E(V-J)/E(B-V) = 2.30$ for comparison purposes; (5) $\Delta E(V-J)$, the difference between the colour excesses in columns (3) and (4); (6) $(A_J)_p$, the total absorption evaluated by the equation $A_J/E(B-V) = 0.87$ and used in the paper; (7) $(A_J)_c$, the total absorption evaluated by the equation $A_J/E(B-V) = 1.70$; and (8) ΔA_J, the difference between the total absorptions in columns (6) and (7).

PASA, 30, e011 (2013)
doi:10.1017/pasa.2012.011

Table 3. J_0 Magnitudes and $(V-J)_0$ Colours for Five Clusters Used for the Absolute Magnitude Calibration

V	$V-J$	J	$(V-J)_0$	J_0	V	$V-J$	J	$(V-J)_0$	J_0	V	$B-V$	$V-I$	V_0	$(B-V)_0$	$V-I_0$	$(V-J)_0$	J_0	$(V-J)_0$	J_0
M92					M13 (cont.)					M67									
12.103	2.332	9.771	2.276	9.749	14.88	1.620	13.260	1.575	13.243	8.740	1.670	2.060	8.622	1.632	2.013	2.808	5.815	2.808	5.815
12.235	2.262	9.973	2.206	9.951	15.036	1.601	13.435	1.556	13.418	8.860	1.590	1.670	8.742	1.552	1.623	2.573	6.169	2.573	6.169
12.362	2.208	10.154	2.152	10.132	15.214	1.569	13.645	1.524	13.628	9.370	1.480	1.500	9.252	1.442	1.453	2.390	6.862	2.390	6.862
12.503	2.147	10.356	2.091	10.334	15.408	1.546	13.862	1.501	13.845	9.530	1.380	1.330	9.412	1.342	1.283	2.218	7.194	2.204	7.373
12.655	2.086	10.569	2.030	10.547	15.585	1.527	14.058	1.482	14.041	9.690	1.360	1.330	9.572	1.322	1.283	2.196	7.376	2.049	8.147
12.798	2.046	10.752	1.990	10.730	15.747	1.511	14.236	1.466	14.219	9.720	1.370	1.360	9.602	1.332	1.313	2.218	7.384	1.897	8.915
12.933	1.999	10.934	1.943	10.912	16.104	1.478	14.626	1.433	14.609	9.840	1.360	1.300	9.722	1.322	1.253	2.185	7.537	1.794	9.382
13.085	1.964	11.121	1.908	11.099	16.433	1.451	14.982	1.406	14.965	10.120	1.300	1.270	10.002	1.262	1.223	2.109	7.894	1.690	10.337
13.236	1.920	11.316	1.864	11.294	16.786	1.424	15.362	1.379	15.345	10.300	1.260	1.230	10.182	1.222	1.183	2.050	8.132	1.585	11.158
13.379	1.889	11.490	1.833	11.468	16.952	1.411	15.541	1.366	15.524	10.520	1.230	1.150	10.402	1.192	1.103	1.987	8.415	–	–
13.528	1.857	11.671	1.801	11.649	17.112	1.397	15.715	1.352	15.698	10.930	1.150	1.140	10.812	1.112	1.093	1.897	8.915	–	–
13.682	1.818	11.864	1.762	11.842	17.271	1.381	15.890	1.336	15.873	11.200	1.080	1.080	11.082	1.042	1.033	1.799	9.283	–	–
13.827	1.783	12.044	1.727	12.022	17.420	1.360	16.060	1.315	16.043	11.240	1.100	1.070	11.122	1.062	1.023	1.817	9.305	–	–
13.984	1.761	12.223	1.705	12.201						11.440	1.060	1.050	11.322	1.022	1.003	1.766	9.556	–	–
					M71														
14.140	1.727	12.413	1.671	12.391	11.997	4.109	7.888	3.479	7.644	12.094	1.007	1.016	11.976	0.969	0.969	1.696	10.280	–	–
14.321	1.692	12.629	1.636	12.607	12.035	3.717	8.318	3.087	8.074	12.110	1.006	1.029	11.992	0.968	0.982	1.700	10.292	–	–
14.541	1.653	12.888	1.597	12.866	12.116	3.469	8.647	2.839	8.403	12.230	0.993	1.002	12.112	0.955	0.955	1.675	10.437	–	–
14.744	1.627	13.117	1.571	13.095	12.212	3.300	8.912	2.670	8.668	12.712	0.913	0.966	12.594	0.875	0.919	1.575	11.019	–	–
14.925	1.595	13.330	1.539	13.308	12.347	3.137	9.210	2.507	8.966	12.862	0.941	0.981	12.744	0.903	0.934	1.611	11.133	–	–
15.089	1.565	13.524	1.509	13.502	12.523	2.962	9.561	2.332	9.317	12.934	0.917	0.972	12.816	0.879	0.925	1.582	11.234	–	–
15.256	1.547	13.709	1.491	13.687	12.693	2.833	9.860	2.203	9.616	12.934	0.919	0.940	12.816	0.881	0.893	1.572	11.244	–	–
15.456	1.525	13.931	1.469	13.909	12.906	2.733	10.173	2.103	9.929	$(V-J)_0$	M_V	V	V_0	$(V-J)_0$	J_0	–	–	–	–
15.637	1.507	14.130	1.451	14.108	13.139	2.648	10.491	2.018	10.247	NGC 6791						–	–	–	–
15.929	1.479	14.450	1.423	14.428	13.305	2.562	10.743	1.932	10.499	2.994	−0.175	13.395	12.930	2.994	9.936	–	–	–	–
16.118	1.463	14.655	1.407	14.633	13.459	2.516	10.943	1.886	10.699	2.935	−0.140	13.430	12.965	2.935	10.030	–	–	–	–
16.292	1.448	14.844	1.392	14.822	13.646	2.465	11.181	1.835	10.937	2.832	−0.078	13.492	13.027	2.832	10.195	–	–	–	–
16.453	1.435	15.018	1.379	14.996	13.818	2.422	11.396	1.792	11.152	2.742	0.007	13.577	13.112	2.742	10.370	–	–	–	–
16.623	1.421	15.202	1.365	15.180	13.993	2.381	11.612	1.751	11.368	2.671	0.085	13.655	13.190	2.671	10.519	–	–	–	–
16.801	1.406	15.395	1.350	15.373	14.177	2.342	11.835	1.712	11.591	2.592	0.197	13.767	13.302	2.592	10.710	–	–	–	–
16.970	1.391	15.579	1.335	15.557	14.356	2.306	12.050	1.676	11.806	2.514	0.295	13.865	13.400	2.514	10.886	–	–	–	–
17.130	1.376	15.754	1.320	15.732	14.538	2.274	12.264	1.644	12.020	2.443	0.422	13.992	13.527	2.443	11.084	–	–	–	–
17.279	1.368	15.911	1.312	15.889	14.736	2.247	12.489	1.617	12.245	2.376	0.541	14.111	13.646	2.376	11.270	–	–	–	–
M13					14.986	2.209	12.777	1.579	12.533	2.328	0.647	14.217	13.752	2.328	11.424	–	–	–	–
11.895	2.729	9.166	2.684	9.1486	15.217	2.177	13.040	1.547	12.796	2.280	0.766	14.336	13.871	2.280	11.591	–	–	–	–
12.005	2.612	9.393	2.567	9.3756	15.426	2.152	13.274	1.522	13.030	2.221	0.899	14.469	14.004	2.221	11.783	–	–	–	–
12.152	2.474	9.678	2.429	9.6606	15.627	2.120	13.507	1.490	13.263	2.167	1.054	14.624	14.159	2.167	11.992	–	–	–	–
12.289	2.373	9.916	2.328	9.8986	15.854	2.080	13.774	1.450	13.530	2.124	1.180	14.750	14.285	2.124	12.161	–	–	–	–
12.487	2.258	10.229	2.213	10.212	16.060	2.070	13.990	1.440	13.746	2.088	1.307	14.877	14.412	2.088	12.324	–	–	–	–
12.642	2.182	10.460	2.137	10.443	16.268	2.035	14.233	1.405	13.989	2.040	1.461	15.031	14.566	2.040	12.526	–	–	–	–
12.787	2.104	10.683	2.059	10.666	16.485	2.021	14.464	1.391	14.220	2.010	1.616	15.186	14.721	2.010	12.711	–	–	–	–
12.923	2.053	10.870	2.008	10.853	16.688	1.989	14.699	1.359	14.455	1.986	1.735	15.305	14.840	1.986	12.854	–	–	–	–
13.051	1.999	11.052	1.954	11.035	16.885	1.977	14.908	1.347	14.664	1.963	1.862	15.432	14.967	1.963	13.004	–	–	–	–
13.211	1.944	11.267	1.899	11.25	17.084	1.959	15.125	1.329	14.881	1.933	2.002	15.572	15.107	1.933	13.174	–	–	–	–
13.36	1.907	11.453	1.862	11.436	17.267	1.931	15.336	1.301	15.092	1.909	2.150	15.720	15.255	1.909	13.346	–	–	–	–
13.499	1.875	11.624	1.830	11.607	–	–	–	–	–	1.878	2.297	15.867	15.402	1.878	13.524	–	–	–	–
13.646	1.843	11.803	1.798	11.786	–	–	–	–	–	1.842	2.445	16.015	15.550	1.842	13.708	–	–	–	–
13.800	1.802	11.998	1.757	11.981	–	–	–	–	–	1.830	2.606	16.176	15.711	1.830	13.881	–	–	–	–
13.945	1.774	12.171	1.729	12.154	–	–	–	–	–	1.800	2.782	16.352	15.887	1.800	14.087	–	–	–	–
14.088	1.748	12.340	1.703	12.323	–	–	–	–	–	1.782	2.993	16.563	16.098	1.782	14.316	–	–	–	–
14.238	1.722	12.516	1.677	12.499	–	–	–	–	–	1.764	3.161	16.731	16.266	1.764	14.502	–	–	–	–
14.393	1.697	12.696	1.652	12.679	–	–	–	–	–	1.746	3.380	16.950	16.485	1.746	14.739	–	–	–	–
14.546	1.667	12.879	1.622	12.862	–	–	–	–	–	1.728	3.520	17.090	16.625	1.728	14.897	–	–	–	–
14.715	1.643	13.072	1.598	13.055	–	–	–	–	–	1.722	3.682	17.252	16.787	1.722	15.065	–	–	–	–

Note. The last two columns for the cluster M67 indicate the $(V-I)_0$ colours and J_0 magnitudes of the bins used to draw the diagram of M67 in Figure 1.

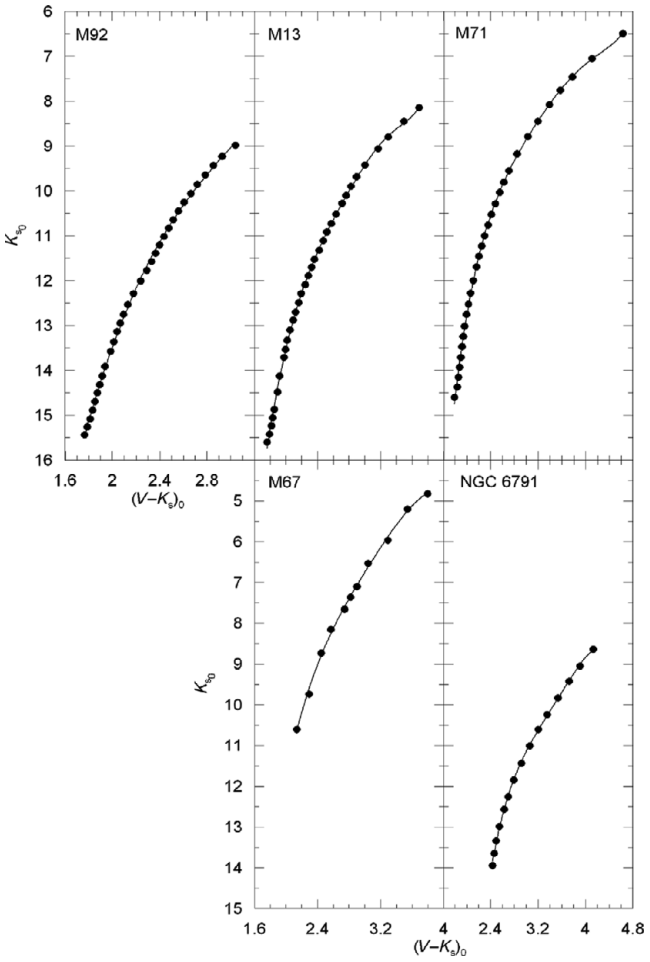

Figure 2. $K_{s_0} \times (V - K_s)_0$ colour–apparent magnitude diagrams for five Galactic clusters used for the absolute magnitude calibration.

from Paper I. These data are given in Table 1, whereas the J_0 magnitudes and $(V - J)_0$ colours are presented in Table 3. We then fitted the fiducial sequence of the red giants to a fourth-degree polynomial for all clusters. The calibration of J_0 is as follows:

$$J_0 = \sum_{i=0}^{4} a_i (V - J)_0^i. \quad (2)$$

The numerical values of the coefficients a_i ($i = 1, 2, 3, 4$) are given in Table 4 and the corresponding diagrams are presented in Figure 1. The $(V - J)_0$ interval in the second line of the table denotes the range of $(V - J)_0$ available for each cluster.

2.2 Data for Calibration with K_{s_0} and $(V - K_s)_0$

We used the data of the same clusters as mentioned in Section 2.1, i.e. M92, M13, M71, M67, and NGC 6791, for calibration of the M_{K_s} absolute magnitudes. We adopted the same colour excesses, distance moduli, and metallicities as in Table 1. The K_{s_0} magnitudes and $(V - K_s)_0$ colours for the clusters M92, M13, and M71 were taken from the tables of Brasseur et al. (2010). However, we used two different procedures for evaluation of the K_s and $V - K_s$ data for the clusters M67 and NGC 6791, as explained in the following. For the cluster M67, we transformed the V, $B - V$, and $V - I$ data of Montgomery et al. (1993) to $(V - K_s)_0$ by the following equation of Yaz et al. (2010), and then we evaluated the K_{s_0} magnitudes by the combination of V_0 magnitudes and $(V - K_s)_0$ colours:

$$(V - K_s)_0 = 1.791(B - V)_0 + 0.294(V - I)_0 - 0.129[\mathrm{Fe/H}] + 0.279. \quad (3)$$

The available 2MASS photometric data in Brasseur et al. (2010) for the cluster NGC 6791 are the $J - K_s$ colours and K_s magnitudes, but not the $V - K_s$ ones. Hence, we evaluated them by means of the V_0 and J_0 magnitudes for this cluster given in Table 3 in three steps. First, we plotted V_0 magnitudes versus J_0 magnitudes in a diagram (not given here) and obtained the following quadratic equation with a high correlation coefficient, $R^2 = 0.9997$:

$$V_0 = 0.0457 J_0^2 - 0.3744 J_0 + 12.9000. \quad (4)$$

In the second step, we evaluated the J magnitudes by combining $J - K_s$ and K_s, and finally we de-reddened the J magnitudes and transformed them to V_0 magnitudes by Equation (4). We used the equations $A_J/E(B - V) = 0.87$ and $A_{K_s}/E(B - V) = 0.38$ of Savage & Mathis (1979) for de-reddening of the magnitudes J and K_s, respectively. As Equation (4) is defined for $9.94 \leq J_0 \leq 15.06$, we could not consider five bright J_0 magnitudes in Table 3. The $(V - K_s)_0$ and K_{s_0} data for the clusters are given in Table 5.

As in Section 2.1, we adopted different equations, i.e. $R = A_V/E(B - V) = 4.0$ (Turner 2012), $E(J - H)/E(B - V) =$

Table 4. Numerical Values of the Coefficients a_i ($i = 1, 2, 3, 4$) in Equation (2)

Cluster →	M92	M13	M71	M67	NGC 6791
$(V - J)_0$	[1.30, 2.28]	[1.30, 2.68]	[1.30, 3.48]	[1.58, 2.81]	[1.72, 2.99]
a_4	8.7460	2.1654	0.5646	3.0424	3.4182
a_3	− 67.6790	− 20.4910	− 6.5667	− 27.8780	− 34.682
a_2	198.3500	73.7370	28.9320	97.1910	132.690
a_1	− 265.4200	− 121.9800	− 58.6600	− 156.3900	− 229.450
a_0	149.6300	89.1650	55.3480	106.7000	163.660

PASA, 30, e011 (2013)
doi:10.1017/pasa.2012.011

Table 5. K_{s_0} Magnitudes and $(V-K_s)_0$ Colours for Five Clusters Used for the Absolute Magnitude Calibration

V	$V-K_s$	K_s	$(V-K_s)_0$	K_{s_0}	V	$V-K_s$	K_s	$(V-K_s)_0$	K_{s_0}					
		M92					M71 (cont.)							
12.103	3.108	8.995	3.039	8.9855	12.347	4.164	8.183	3.391	8.077	–	–	–	–	–
12.235	2.998	9.237	2.929	9.2275	12.523	3.970	8.553	3.197	8.447	–	–	–	–	–
12.362	2.922	9.440	2.853	9.4305	12.693	3.800	8.893	3.027	8.787	–	–	–	–	–
12.503	2.854	9.649	2.785	9.6395	12.906	3.619	9.287	2.846	9.181	–	–	–	–	–
12.655	2.787	9.868	2.718	9.8585	13.139	3.481	9.658	2.708	9.552	–	–	–	–	–
12.798	2.730	10.068	2.661	10.059	13.305	3.390	9.915	2.617	9.809	–	–	–	–	–
12.933	2.675	10.258	2.606	10.249	13.459	3.324	10.135	2.551	10.029	–	–	–	–	–
13.085	2.626	10.459	2.557	10.450	13.646	3.250	10.396	2.477	10.290	–	–	–	–	–
13.236	2.583	10.653	2.514	10.644	13.818	3.187	10.631	2.414	10.525	–	–	–	–	–
13.379	2.544	10.835	2.475	10.826	13.993	3.129	10.864	2.356	10.758	–	–	–	–	–
13.528	2.505	11.023	2.436	11.014	14.177	3.071	11.106	2.298	11.000	–	–	–	–	–
13.682	2.467	11.215	2.398	11.206	14.356	3.020	11.336	2.247	11.230	–	–	–	–	–
13.827	2.433	11.394	2.364	11.385	14.538	2.974	11.564	2.201	11.458	–	–	–	–	–
13.984	2.399	11.585	2.330	11.576	14.736	2.935	11.801	2.162	11.695	–	–	–	–	–
14.140	2.357	11.783	2.288	11.774	14.986	2.880	12.106	2.107	12.000	–	–	–	–	–
14.321	2.308	12.013	2.239	12.004	15.217	2.835	12.382	2.062	12.276	–	–	–	–	–
14.541	2.247	12.294	2.178	12.285	15.426	2.798	12.628	2.025	12.522	–	–	–	–	–
14.744	2.201	12.543	2.132	12.534	15.627	2.766	12.861	1.993	12.755	–	–	–	–	–
14.925	2.162	12.763	2.093	12.754	15.854	2.734	13.120	1.961	13.014	–	–	–	–	–
15.089	2.136	12.953	2.067	12.944	16.060	2.709	13.351	1.936	13.245	–	–	–	–	–
15.256	2.109	13.147	2.040	13.138	16.268	2.687	13.581	1.914	13.475	–	–	–	–	–
15.456	2.080	13.376	2.011	13.367	16.485	2.667	13.818	1.894	13.712	–	–	–	–	–
15.637	2.054	13.583	1.985	13.574	16.688	2.649	14.039	1.876	13.933	–	–	–	–	–
15.929	2.005	13.924	1.936	13.915	16.885	2.631	14.254	1.858	14.148	–	–	–	–	–
16.118	1.982	14.136	1.913	14.127	17.084	2.606	14.478	1.833	14.372	–	–	–	–	–
16.292	1.961	14.331	1.892	14.322	17.267	2.564	14.703	1.791	14.597	–	–	–	–	–
16.453	1.942	14.511	1.873	14.502	$J-K_s$	K_s	J	J_0	V_0	K_{s_0}	$(V-K_s)_0$			
16.623	1.922	14.701	1.853	14.692				NGC 6791					–	–
16.801	1.901	14.900	1.832	14.891	1.111	8.693	9.804	9.717	12.767	8.636	4.131	–	–	–
16.970	1.880	15.090	1.811	15.081	1.060	9.103	10.163	10.076	12.957	9.046	3.911	–	–	–
17.130	1.857	15.273	1.788	15.264	1.016	9.478	10.494	10.407	13.143	9.421	3.722	–	–	–
17.279	1.832	15.447	1.763	15.438	0.978	9.887	10.865	10.778	13.363	9.830	3.533	–	–	–
		M13			0.930	10.297	11.227	11.140	13.591	10.240	3.351	–	–	–
11.895	3.741	8.154	3.686	8.146	0.901	10.661	11.562	11.475	13.811	10.604	3.207	–	–	–

https://doi.org/10.1017/pasa.2012.011 Published online by Cambridge University Press

PASA, 30, e011 (2013)
doi:10.1017/pasa.2012.011

Table 5. Continued.

V	$V-K_s$	K_s	$(V-K_s)_0$	K_{s_0}	V	$V-K_s$	K_s	$(V-K_s)_0$	K_{s_0}					
		M92					M71 (cont.)							
12.005	3.547	8.458	3.492	8.450	0.870	11.060	11.930	11.843	14.066	11.003	3.063	–	–	–
12.152	3.352	8.800	3.297	8.792	0.835	11.493	12.328	12.241	14.355	11.436	2.919	–	–	–
12.289	3.223	9.066	3.168	9.058	0.800	11.903	12.703	12.616	14.640	11.846	2.794	–	–	–
12.487	3.058	9.429	3.003	9.421	0.784	12.312	13.096	13.009	14.953	12.255	2.698	–	–	–
12.642	2.952	9.690	2.897	9.682	0.762	12.617	13.379	13.292	15.188	12.560	2.628	–	–	–
12.787	2.880	9.907	2.825	9.899	0.739	13.039	13.778	13.691	15.530	12.982	2.548	–	–	–
12.923	2.818	10.105	2.763	10.097	0.721	13.390	14.111	14.024	15.827	13.333	2.494	–	–	–
13.051	2.768	10.283	2.713	10.275	0.708	13.705	14.413	14.326	16.106	13.648	2.458	–	–	–
13.211	2.689	10.522	2.634	10.514	0.701	13.999	14.700	14.613	16.378	13.942	2.436	–	–	–
13.360	2.628	10.732	2.573	10.724	1.168	8.225	9.393	9.306	–	–	–	–	–	–
13.499	2.573	10.926	2.518	10.918	1.229	7.768	8.997	8.910	–	–	–	–	–	–
13.646	2.529	11.117	2.474	11.109	1.276	7.453	8.729	8.642	–	–	–	–	–	–
13.800	2.475	11.325	2.420	11.317	1.330	7.124	8.454	8.367	–	–	–	–	–	–
13.945	2.415	11.530	2.360	11.522	1.362	6.901	8.263	8.176	–	–	–	–	–	–
14.088	2.379	11.709	2.324	11.701	V	$B-V$	$V-I$	V_0	$(B-V)_0$	$(V-I)_0$	$(V-K_s)_0$	K_s	$(V-K_s)_0$	K_{s_0}
14.238	2.342	11.896	2.287	11.888						M67				
14.393	2.298	12.095	2.243	12.087	8.740	1.670	2.060	8.622	1.632	2.013	3.796	4.826	2.135	10.608
14.546	2.249	12.297	2.194	12.289	8.860	1.590	1.670	8.742	1.552	1.623	3.538	5.204	2.292	9.735
14.715	2.215	12.500	2.160	12.492	9.370	1.480	1.500	9.252	1.442	1.453	3.291	5.961	2.447	8.729
14.880	2.173	12.707	2.118	12.699	9.530	1.380	1.330	9.412	1.342	1.283	3.062	6.350	2.570	8.157
15.036	2.145	12.891	2.090	12.883	9.690	1.360	1.330	9.572	1.322	1.283	3.026	6.546	2.740	7.662
15.214	2.104	13.110	2.049	13.102	9.720	1.370	1.360	9.602	1.332	1.313	3.053	6.550	2.817	7.365
15.408	2.072	13.336	2.017	13.328	9.840	1.360	1.300	9.722	1.322	1.253	3.017	6.705	2.901	7.101
15.585	2.050	13.535	1.995	13.527	10.120	1.300	1.270	10.002	1.262	1.223	2.901	7.101	3.039	6.538
15.747	2.031	13.716	1.976	13.708	10.300	1.260	1.230	10.182	1.222	1.183	2.817	7.365	3.291	5.961
16.104	1.974	14.130	1.919	14.122	10.520	1.230	1.150	10.402	1.192	1.103	2.740	7.662	3.538	5.204
16.433	1.945	14.488	1.890	14.480	10.930	1.150	1.140	10.812	1.112	1.093	2.594	8.218	3.796	4.826
16.786	1.907	14.879	1.852	14.871	11.200	1.080	1.080	11.082	1.042	1.033	2.451	8.631	–	–
16.952	1.888	15.064	1.833	15.056	11.240	1.100	1.070	11.122	1.062	1.023	2.484	8.638	–	–
17.112	1.868	15.244	1.813	15.236	11.440	1.060	1.050	11.322	1.022	1.003	2.406	8.916	–	–
17.271	1.844	15.427	1.789	15.419	12.094	1.007	1.016	11.976	0.969	0.969	2.301	9.675	–	–
17.420	1.814	15.606	1.759	15.598	12.110	1.006	1.029	11.992	0.968	0.982	2.303	9.689	–	–
		M71			12.230	0.993	1.002	12.112	0.955	0.955	2.272	9.840	–	–
11.997	5.401	6.596	4.628	6.490	12.712	0.913	0.966	12.594	0.875	0.919	2.118	10.476	–	–
12.035	4.883	7.152	4.110	7.046	12.862	0.941	0.981	12.744	0.903	0.934	2.173	10.571	–	–
12.116	4.552	7.564	3.779	7.458	12.934	0.917	0.972	12.816	0.879	0.925	2.127	10.689	–	–
12.212	4.350	7.862	3.577	7.756	12.934	0.919	0.940	12.816	0.881	0.893	2.121	10.695	–	–

Note. The last two columns for the cluster M67 indicate the $(V-K_s)_0$ colours and K_{s_0} magnitudes of the bins used to draw the diagram of M67 in Figure 2.

Table 6. Comparison of the Selective and Total Absorptions Evaluated by Using Different Extinction and Colour Excess Ratios

(1) Cluster	(2) $E(B-V)$	(3) $E(V-K_s)_p$	(4) $E(V-K_s)_c$	(5) $\Delta E(V-K_s)$	(6) $(A_{K_s})_p$	(7) $(A_{K_s})_c$	(8) ΔA_{K_s}
M92	0.025	0.068	0.069	0.001	0.010	0.032	0.022
M13	0.020	0.054	0.055	0.001	0.008	0.025	0.018
M71	0.280	0.762	0.767	0.005	0.106	0.353	0.246
M67	0.038	0.103	0.104	0.001	0.014	0.048	0.033
NGC 6791	0.150	0.408	0.411	0.003	0.057	0.189	0.132

Notes. Description of columns: (1) the cluster; (2) adopted $E(B-V)$ colour excess; (3) $E(V-K_s)_p$, the colour excess evaluated by the equation $E(V-K_s)/E(B-V)=2.72$ used in the paper; (4) $E(V-K_s)_c$, the colour excess evaluated by the equation $E(V-K_s)/E(B-V)=2.74$ for comparison purposes; (5) $\Delta E(V-K_s)$, the difference between the colour excesses in columns (3) and (4); (6) $(A_{K_s})_p$, the total absorption evaluated by the equation $A_{K_s}/E(B-V)=0.38$ used in the paper; (7) $(A_{K_s})_c$, the total absorption evaluated by the equation $A_{K_s}/E(B-V)=1.26$; and (8) ΔA_{K_s}, the difference between the total absorptions in columns (6) and (7).

Table 7. Numerical Values of the Coefficients b_i ($i=1,\ 2,\ 3,\ 4,\ 5$) in Equation (5)

Cluster →	M92	M13	M71*	M67	NGC 6791
$(V-K_s)_0$ →	[1.76, 3.04]	[1.76, 3.69]	[1.79, 3.10]	[2.14, 3.80]	[2.44, 4.13]
b_5	–	–	–	1.5121	–
b_4	2.2478	0.9441	0.3976	− 21.290	1.2082
b_3	− 22.7640	− 11.2930	− 5.6464	117.700	− 16.8610
b_2	87.9930	51.2230	30.0540	− 317.680	88.1870
b_1	− 157.9500	− 106.9700	− 72.7860	412.050	− 207.2100
b_0	123.5300	97.8320	76.9680	− 191.240	196.4700

*The $(V-K_s)_0$ domain of the cluster M71 is in fact [1.79, 4.63]. However, we restricted it with an upper limit of 3.10 mag due to some uncertainties claimed by the authors.

0.295, $E(H-K_s)/E(J-H)=0.49$ (Turner 2011), and evaluated the corresponding $E(V-K_s)=2.74E(B-V)$ selective and $A_{K_s}=1.26E(B-V)$ total absorptions for the clusters. The results are given in Table 6. The differences in $E(V-K_s)$ and ΔA_{K_s} are almost the same as in Table 2. We prefer the extinction ratio and the colour excess ratios used in our study due to the reason explained in Section 2.1.

We fitted the $(V-K_s)_0$ colours and K_{s0} magnitudes to a fourth-degree polynomial for all clusters, except M67 for which a fifth-degree polynomial provided a higher correlation coefficient. The calibration of K_{s_0} is as follows:

$$K_{s_0}=\sum_{i=0}^{5} b_i (V-K_s)_0^i. \tag{5}$$

The numerical values of the coefficients b_i ($i=1,\ 2,\ 3,\ 4,\ 5$) are given in Table 7 and the corresponding diagrams are presented in Figure 2. The $(V-K_s)_0$ interval in the second line of the table indicates the range of $(V-K_s)_0$ available for each cluster.

3 THE PROCEDURE

3.1 Absolute Magnitude as a Function of Metallicity

We adopted the procedure in Paper II, which consists of calibration of an absolute magnitude as a function of metallicity. We calibrated the M_J and M_{K_s}, absolute magnitudes in terms of metallicity for a given $(V-J)_0$ and $(V-K_s)_0$ colour, respectively.

3.1.1 Calibration of M_J in Terms of Metallicity

We estimated the M_J absolute magnitudes for the $(V-J)_0$ colours given in Table 8 for the clusters M92, M13, M71, M67, and NGC 6791 by combining the J_0 apparent magnitudes evaluated by using Equation (2) and the true distance modulus (μ_0) of the cluster in question, i.e.

$$M_J=J_0-\mu_0. \tag{6}$$

Then, we plotted the absolute magnitudes versus $(V-J)_0$ colours. Figure 3 shows that the absolute magnitude is metallicity dependent. It increases (algebraically) with increasing metallicity and decreasing colour.

Now, we can fit the M_J absolute magnitudes to the corresponding [Fe/H] metallicity for a given $(V-J)_0$ colour index and obtain the required calibration. This is carried out for the colour indices $(V-J)_0=1.30$, 1.60, 1.90, 2.10, 2.25, 2.50, and 2.65 mag just for exhibition of the procedure. The results are given in Table 9 and Figure 4. The absolute magnitudes in all colour indices could be fitted to quadratic polynomials with high (squared) correlation coefficients, i.e. $R^2\geq 0.9982$, including $(V-J)_0=1.90$, 2.10, and 2.25 mag, which cover the largest metallicity range, $-2.15\leq$ [Fe/H] $\leq +0.37$ dex. A high correlation coefficient plus (relatively) polynomial

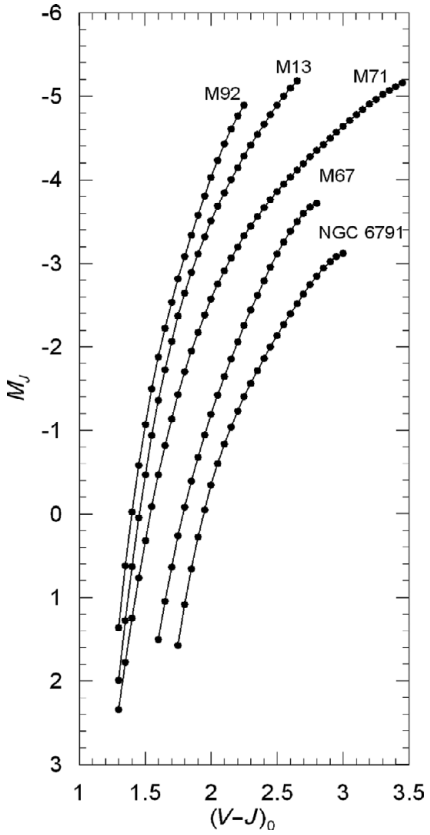

Figure 3. $M_J \times (V-J)_0$ colour–absolute magnitude diagrams for five clusters used for the absolute magnitude calibration.

with small degree is a strong clue for accurate absolute magnitude estimation.

This procedure can be applied to any $(V-J)_0$ colour interval for which the sample clusters are defined. The $(V-J)_0$ domain of the clusters is different. Hence, we adopted this interval as $1.3 \leq (V-J)_0 \leq 2.8$ mag, where at least two clusters are defined, and we evaluated M_J absolute magnitude for each colour. Here, $1.72 \leq (V-J)_0 \leq 2.28$ mag is the interval where all the clusters are defined, whereas the range of the interval where only two clusters (M67 and NGC 6791) are defined is rather small, i.e. $2.69 \leq (V-J)_0 \leq 2.80$ mag. However, this small interval can be used for estimation of the absolute magnitudes for red giants with metallicities $-0.04 \leq$ [Fe/H] $\leq +0.37$ dex. The general form of the equation for the calibration is as follows:

$$M_J = c_0 + c_1 X + c_2 X^2, \tag{7}$$

where $X =$ [Fe/H]. M_J could be fitted in terms of metallicity by a quadratic polynomial for all $(V-J)_0$ colour intervals with a high correlation coefficient, $R^2 \geq 0.996$, except two intervals with small ranges, i.e. a linear fitting was sufficient for the colour intervals $1.34 \leq (V-J)_0 \leq 1.41$ and $2.69 \leq (V-J)_0 \leq 2.80$ mag where only two clusters are defined. The absolute magnitudes estimated via Equation (7) for 151 $(V-J)_0$ colour indices and the corresponding $c_i (i = 0, 1, 2)$ coefficients are given in Table 10. However, the diagrams for the calibrations are not given in the paper because of space constraints.

Table 8. M_J Absolute Magnitudes Estimated for a Set of $(V-J)_0$ Colours for Five Clusters Used in the Calibration

Cluster→	M92	M13	M71	M67	NGC 6791
$(V-J)_0$			M_J		
1.30	1.364	1.992	2.341	–	–
1.35	0.620	1.275	1.774	–	–
1.40	– 0.025	0.629	1.251	–	–
1.45	– 0.584	0.049	0.767	–	–
1.50	– 1.073	– 0.472	0.321	–	–
1.55	– 1.501	– 0.938	– 0.091	–	–
1.60	– 1.881	– 1.356	– 0.469	1.505	–
1.65	– 2.222	– 1.731	– 0.817	1.048	–
1.70	– 2.532	– 2.068	– 1.137	0.635	–
1.75	– 2.817	– 2.370	– 1.431	0.261	1.571
1.80	– 3.084	– 2.643	– 1.700	– 0.080	1.083
1.85	– 3.336	– 2.890	– 1.948	– 0.391	0.655
1.90	– 3.576	– 3.114	– 2.175	– 0.678	0.278
1.95	– 3.806	– 3.320	– 2.383	– 0.944	– 0.053
2.00	– 4.026	– 3.509	– 2.574	– 1.192	– 0.345
2.05	– 4.235	– 3.684	– 2.750	– 1.425	– 0.604
2.10	– 4.431	– 3.847	– 2.912	– 1.646	– 0.835
2.15	– 4.609	– 4.001	– 3.061	– 1.857	– 1.042
2.20	– 4.766	– 4.146	– 3.199	– 2.058	– 1.231
2.25	– 4.894	– 4.285	– 3.327	– 2.253	– 1.404
2.30	–	– 4.417	– 3.447	– 2.439	– 1.566
2.35	–	– 4.545	– 3.559	– 2.619	– 1.717
2.40	–	– 4.667	– 3.664	– 2.792	– 1.862
2.45	–	– 4.783	– 3.763	– 2.956	– 2.001
2.50	–	– 4.895	– 3.857	– 3.111	– 2.135
2.55	–	– 5.000	– 3.947	– 3.255	– 2.266
2.60	–	– 5.097	– 4.033	– 3.386	– 2.393
2.65	–	– 5.186	– 4.116	– 3.501	– 2.516
2.70	–	–	– 4.197	– 3.598	– 2.634
2.75	–	–	– 4.275	– 3.672	– 2.745
2.80	–	–	– 4.352	– 3.719	– 2.848
2.85	–	–	– 4.427	–	– 2.940
2.90	–	–	– 4.500	–	– 3.019
2.95	–	–	– 4.572	–	– 3.080
3.00	–	–	– 4.642	–	– 3.120
3.05	–	–	– 4.711	–	–
3.10	–	–	– 4.778	–	–
3.15	–	–	– 4.843	–	–
3.20	–	–	– 4.905	–	–
3.25	–	–	– 4.965	–	–
3.30	–	–	– 5.021	–	–
3.35	–	–	– 5.073	–	–
3.40	–	–	– 5.120	–	–
3.45	–	–	– 5.162	–	–

3.1.2 *Calibration of M_{K_s} in Terms of Metallicity*

We estimated the M_{K_s} absolute magnitudes for the $(V-K_s)_0$ colours given in Table 11 for the clusters M92, M13, M71, M67, and NGC 6791 by combining the K_{s_0} apparent magnitudes evaluated by Equation (5) and the true distance modulus (μ_0) of the cluster in question, i.e.

$$M_{K_s} = K_{s_0} - \mu_0. \tag{8}$$

Table 9. M_J Absolute Magnitudes and [Fe/H] Metallicities for Seven $(V-J)_0$ Intervals

$(V-J)_0$	[Fe/H] (dex)	M_J
1.30	− 2.15	1.364
	− 1.41	1.992
	− 0.78	2.341
1.60	− 2.15	− 1.881
	− 1.41	− 1.356
	− 0.78	− 0.469
	− 0.04	1.505
1.90	− 2.15	− 3.576
	− 1.41	− 3.114
	− 0.78	− 2.175
	− 0.04	− 0.678
	0.37	0.278
2.10	− 2.15	− 4.431
	− 1.41	− 3.847
	− 0.78	− 2.912
	− 0.04	− 1.646
	0.37	− 0.835
2.25	− 2.15	− 4.894
	− 1.41	− 4.285
	− 0.78	− 3.327
	− 0.04	− 2.253
	0.37	− 1.404
2.50	− 1.41	− 4.895
	− 0.04	− 3.111
	0.37	− 2.135
2.65	− 1.41	− 5.186
	− 0.04	− 3.501
	0.37	− 2.516

Then, we plotted the absolute magnitudes versus $(V-K_s)_0$ colours. Figure 5 shows a similar trend of Figure 3, i.e. the absolute magnitude increases (algebraically) with increasing metallicity and decreasing colour.

We fitted the M_{K_s} absolute magnitudes to the corresponding [Fe/H] metallicity for the colour indices $(V-K_s)_0 =$ 1.80, 2.00, 2.20, 2.40, 2.60, 3.00, and 3.30 mag just for the exhibition of the procedure. The results are given in Table 12 and Figure 6. We can extend this fitting to a larger $(V-K_s)_0$ interval for which the sample clusters are defined. The $(V-K_s)_0$ domains of the clusters are different. Hence, we adopted this interval as $1.75 \leq (V-K_s)_0 \leq$ 3.80 mag where at least two clusters are defined. However, the range of the interval where only two clusters are defined is rather limited, i.e. $1.75 \leq (V-K_s)_0 \leq 1.78$ and $3.70 \leq (V-K_s)_0 \leq 3.80$ mag. The common domain of all the clusters is $2.45 \leq (V-K_s)_0 \leq 3.04$ mag. The general form of the equation for the calibration is as follows:

$$M_{K_s} = d_0 + d_1 X + d_2 X^2, \quad (9)$$

where $X =$ [Fe/H]. Note that M_{K_s} could be fitted in terms of metallicity by a quadratic polynomial for all $(V-K_s)_0$ colour intervals with a high correlation coefficient, $R^2 \geq$ 0.9972, except two intervals with small ranges, i.e. a linear fitting was sufficient for the colour intervals $1.75 \leq (V-K_s)_0 \leq 1.78$ and $3.70 \leq (V-K_s)_0 \leq 3.80$ mag where only two clusters are defined. The absolute magnitudes estimated via Equation (9) for 206 $(V-K_s)_0$ colour indices and the corresponding $d_i (i = 0, 1, 2)$ coefficients are given in Table 13. However, the diagrams for the calibrations are not given here because of space constraints.

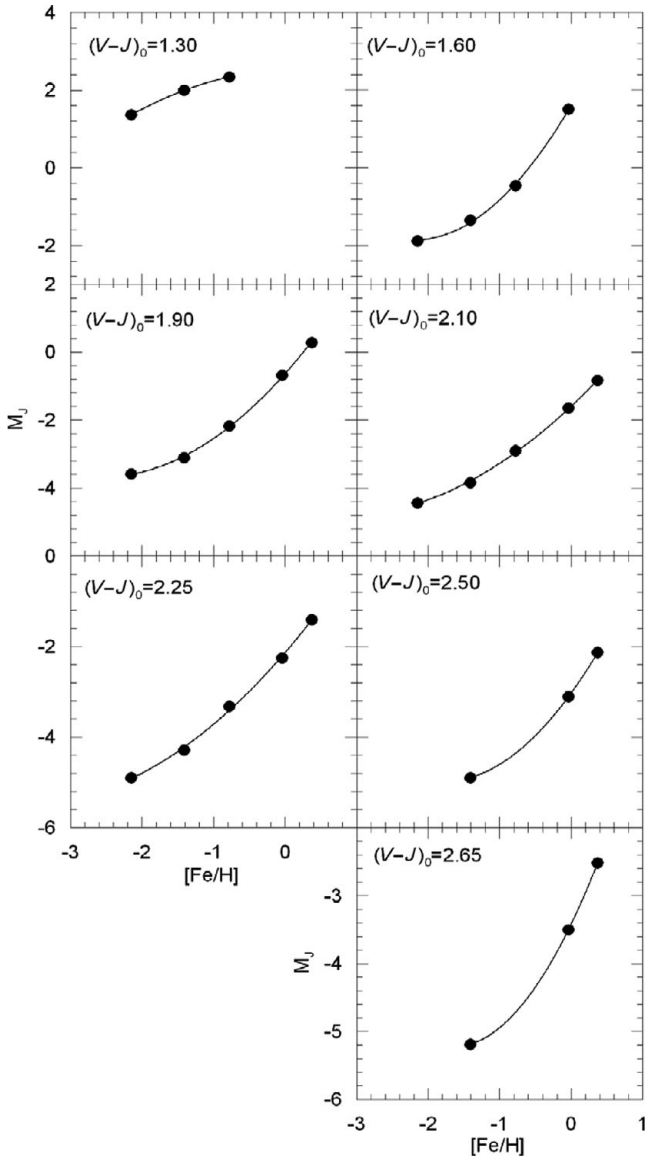

Figure 4. Calibration of the absolute magnitude M_J as a function of metallicity [Fe/H] for seven colour indices.

The calibration of the absolute magnitude M_{K_s} (and M_J) in terms of [Fe/H] is carried out in steps of 0.01 mag. A small step is necessary to isolate an observational error on the colour $V-K_s$ (and $V-J$) plus an error due to reddening. The origin of the errors mentioned is the trend of the RGB. Although they are not as steep as in *BV* and *gr* photometry, a small error in $V-K_s$ (and $V-J$) implies a large change in the absolute magnitude.

https://doi.org/10.1017/pasa.2012.011 Published online by Cambridge University Press

PASA, 30, e011 (2013)
doi:10.1017/pasa.2012.011

Table 10. M_J Absolute Magnitudes Estimated for Five Galactic Clusters and the Numerical Values of c_i ($i = 0, 1, 2$) Coefficients in Equation (7)

Cluster →	M92	M13	M71	M67	NGC 6791						Cluster →	M92	M13	M71	M67	NGC 6791					
$(V-J)_0$			M_J			c_0	c_1	c_2	R^2	[Fe/H] Int.	$(V-J)_0$			M_J			c_0	c_1	c_2	R^2	[Fe/H] Int.
1.30	1.364	1.992	2.341	–	–	2.5339	0.0791	−0.2162	1	[−2.15, −0.78]	2.06	−4.275	−3.717	−2.783	−1.470	−0.652	−1.4238	2.0438	0.3285	0.9991	[−2.15, 0.37]
1.31	1.207	1.843	2.224	–	–	2.4912	0.1978	−0.1859	1	[−2.15, −0.78]	2.07	−4.315	−3.750	−2.816	−1.515	−0.699	−1.4661	2.0284	0.3220	0.9991	[−2.15, 0.37]
1.32	1.054	1.696	2.109	–	–	2.4485	0.3140	−0.1557	1	[−2.15, −0.78]	2.08	−4.354	−3.783	−2.849	−1.559	−0.745	−1.5077	2.0134	0.3156	0.9992	[−2.15, 0.37]
1.33	0.905	1.553	1.996	–	–	2.4057	0.4277	−0.1257	1	[−2.15, −0.78]	2.09	−4.393	−3.815	−2.880	−1.603	−0.790	−1.5486	1.9990	0.3095	0.9992	[−2.15, 0.37]
1.34	0.760	1.412	1.884	–	–	2.5413	0.8220	–	0.9979	[−2.15, −0.78]	2.10	−4.431	−3.847	−2.912	−1.646	−0.835	−1.5888	1.9851	0.3037	0.9992	[−2.15, 0.37]
1.35	0.620	1.275	1.774	–	–	2.4436	0.8438	–	0.9990	[−2.15, −0.78]	2.11	−4.468	−3.879	−2.943	−1.689	−0.878	−1.6284	1.9717	0.2981	0.9992	[−2.15, 0.37]
1.36	0.484	1.140	1.666	–	–	2.3464	0.8639	–	0.9997	[−2.15, −0.78]	2.12	−4.504	−3.910	−2.973	−1.731	−0.920	−1.6675	1.9587	0.2927	0.9992	[−2.15, 0.37]
1.37	0.351	1.008	1.560	–	–	2.2497	0.8825	–	1	[−2.15, −0.78]	2.13	−4.540	−3.940	−3.003	−1.773	−0.962	−1.7059	1.9463	0.2876	0.9992	[−2.15, 0.37]
1.38	0.222	0.879	1.455	–	–	2.1535	0.8995	–	0.9999	[−2.15, −0.78]	2.14	−4.575	−3.971	−3.032	−1.815	−1.002	−1.7439	1.9343	0.2828	0.9992	[−2.15, 0.37]
1.39	0.097	0.752	1.352	–	–	2.0579	0.9152	–	0.9996	[−2.15, −0.78]	2.15	−4.609	−4.001	−3.061	−1.857	−1.042	−1.7813	1.9228	0.2782	0.9992	[−2.15, 0.37]
1.40	−0.025	0.629	1.251	–	–	1.9629	0.9294	–	0.9990	[−2.15, −0.78]	2.16	−4.642	−4.030	−3.090	−1.898	−1.081	−1.8182	1.9118	0.2740	0.9992	[−2.15, 0.37]
1.41	−0.143	0.508	1.151	–	–	1.8686	0.9424	–	0.9982	[−2.15, −0.78]	2.17	−4.675	−4.060	−3.118	−1.938	−1.120	−1.8547	1.9012	0.2700	0.9991	[−2.15, 0.37]
1.42	−0.258	0.389	1.053	–	–	2.0168	1.3377	0.1301	1	[−2.15, −0.78]	2.18	−4.706	−4.089	−3.145	−1.979	−1.158	−1.8907	1.8911	0.2664	0.9991	[−2.15, 0.37]
1.43	−0.370	0.273	0.956	–	–	1.9728	1.4259	0.1564	1	[−2.15, −0.78]	2.19	−4.736	−4.118	−3.172	−2.019	−1.195	−1.9263	1.8815	0.2632	0.9990	[−2.15, 0.37]
1.44	−0.478	0.160	0.861	–	–	1.9286	1.5114	0.1823	1	[−2.15, −0.78]	2.20	−4.766	−4.146	−3.199	−2.058	−1.231	−1.9615	1.8724	0.2603	0.9990	[−2.15, 0.37]
1.45	−0.584	0.049	0.767	–	–	1.8843	1.5943	0.2075	1	[−2.15, −0.78]	2.21	−4.794	−4.175	−3.226	−2.098	−1.267	−1.9963	1.8638	0.2578	0.9989	[−2.15, 0.37]
1.46	−0.687	−0.060	0.675	–	–	1.8397	1.6746	0.2322	1	[−2.15, −0.78]	2.22	−4.821	−4.203	−3.252	−2.137	−1.302	−2.0308	1.8857	0.2557	0.9987	[−2.15, 0.37]
1.47	−0.787	−0.166	0.584	–	–	1.7949	1.7523	0.2564	1	[−2.15, −0.78]	2.23	−4.846	−4.230	−3.277	−2.176	−1.337	−2.0649	1.8480	0.2540	0.9986	[−2.15, 0.37]
1.48	−0.885	−0.270	0.495	–	–	1.7498	1.8273	0.2799	1	[−2.15, −0.78]	2.24	−4.871	−4.258	−3.303	−2.214	−1.371	−2.0987	1.8409	0.2527	0.9985	[−2.15, 0.37]
1.49	−0.980	−0.372	0.407	–	–	1.7046	1.8997	0.3028	1	[−2.15, −0.78]	2.25	−4.894	−4.285	−3.327	−2.253	−1.404	−2.1322	1.8343	0.2519	0.9983	[−2.15, 0.37]
1.50	−1.073	−0.472	0.321	–	–	1.6590	1.9694	0.3251	1	[−2.15, −0.78]	2.26	−4.915	−4.312	−3.352	−2.290	−1.437	−2.1654	1.8282	0.2516	0.9981	[−2.15, 0.37]
1.51	−1.163	−0.569	0.236	–	–	1.6133	2.0366	0.3467	1	[−2.15, −0.78]	2.27	−4.935	−4.339	−3.376	−2.328	−1.470	−2.1984	1.8226	0.2517	0.9979	[−2.15, 0.37]
1.52	−1.251	−0.664	0.152	–	–	1.5673	2.1011	0.3677	1	[−2.15, −0.78]	2.28	−4.954	−4.365	−3.400	−2.365	−1.502	−2.2311	1.8176	0.2524	0.9976	[−2.15, 0.37]
1.53	−1.336	−0.758	0.070	–	–	1.5210	2.1630	0.3879	1	[−2.15, −0.78]	2.29	–	−4.391	−3.424	−2.403	−1.534	−2.2417	1.7305	0.1585	0.9965	[−1.41, 0.37]
1.54	−1.420	−0.849	−0.011	–	–	1.4745	2.2223	0.4075	1	[−2.15, −0.78]	2.30	–	−4.417	−3.447	−2.439	−1.566	−2.2734	1.7244	0.1577	0.9960	[−1.41, 0.37]
1.55	−1.501	−0.938	−0.091	–	–	1.4277	2.2791	0.4264	1	[−2.15, −0.78]	2.31	–	−4.443	–	−2.476	−1.597	−2.3960	2.0134	0.3982	1	[−1.41, 0.37]
1.56	−1.581	−1.025	−0.169	–	–	1.3806	2.3332	0.4445	1	[−2.15, −0.78]	2.32	–	−4.469	–	−2.512	−1.627	−2.4319	2.0230	0.4102	1	[−1.41, 0.37]
1.57	−1.659	−1.111	−0.246	–	–	1.3333	2.3849	0.4620	1	[−2.15, −0.78]	2.33	–	−4.494	–	−2.548	−1.658	−2.4675	2.0328	0.4222	1	[−1.41, 0.37]
1.58	−1.735	−1.194	−0.321	1.702	–	1.8084	3.2112	0.7317	0.9984	[−2.15, −0.04]	2.34	–	−4.520	–	−2.584	−1.688	−2.5029	2.0426	0.4342	1	[−1.41, 0.37]
1.59	−1.809	−1.276	−0.396	1.603	–	1.7099	3.1824	0.7231	0.9987	[−2.15, −0.04]	2.35	–	−4.545	–	−2.619	−1.717	−2.5379	2.0525	0.4463	1	[−1.41, 0.37]
1.60	−1.881	−1.356	−0.469	1.505	–	1.6134	3.1544	0.7148	0.9989	[−2.15, −0.04]	2.36	–	−4.569	–	−2.654	−1.747	−2.5726	2.0624	0.4583	1	[−1.41, 0.37]
1.61	−1.952	−1.435	−0.541	1.410	–	1.5188	3.1272	0.7069	0.9991	[−2.15, −0.04]	2.37	–	−4.594	–	−2.689	−1.776	−2.6070	2.0723	0.4702	1	[−1.41, 0.37]
1.62	−2.022	−1.511	−0.612	1.317	–	1.4262	3.1008	0.6992	0.9993	[−2.15, −0.04]	2.38	–	−4.618	–	−2.724	−1.805	−2.6412	2.0821	0.4821	1	[−1.41, 0.37]
1.63	−2.090	−1.586	−0.682	1.225	–	1.3354	3.0752	0.6918	0.9995	[−2.15, −0.04]	2.39	–	−4.643	–	−2.758	−1.833	−2.6750	2.0917	0.4938	1	[−1.41, 0.37]
1.64	−2.157	−1.659	−0.750	1.136	–	1.2464	3.0502	0.6846	0.9996	[−2.15, −0.04]	2.40	–	−4.667	–	−2.792	−1.862	−2.7085	2.1013	0.5053	1	[−1.41, 0.37]
1.65	−2.222	−1.731	−0.817	1.048	–	1.1592	3.0258	0.6777	0.9997	[−2.15, −0.04]	2.41	–	−4.690	–	−2.825	−1.890	−2.7417	2.1106	0.5167	1	[−1.41, 0.37]
1.66	−2.286	−1.801	−0.883	0.962	–	1.0737	3.0019	0.6709	0.9998	[−2.15, −0.04]	2.42	–	−4.714	–	−2.859	−1.918	−2.7746	2.1197	0.5278	1	[−1.41, 0.37]
1.67	−2.349	−1.870	−0.948	0.878	–	0.9899	2.9786	0.6642	0.9999	[−2.15, −0.04]	2.43	–	−4.737	–	−2.891	−1.946	−2.8072	2.1286	0.5388	1	[−1.41, 0.37]
1.68	−2.411	−1.937	−1.012	0.795	–	0.9078	2.9558	0.6577	0.9999	[−2.15, −0.04]	2.44	–	−4.761	–	−2.924	−1.973	−2.8394	2.1372	0.5494	1	[−1.41, 0.37]
1.69	−2.472	−2.003	−1.075	0.714	–	0.8272	2.9333	0.6513	1	[−2.15, −0.04]	2.45	–	−4.783	–	−2.956	−2.001	−2.8713	2.1454	0.5597	1	[−1.41, 0.37]
1.70	−2.532	−2.068	−1.137	0.635	–	0.7482	2.9113	0.6449	1	[−2.15, −0.04]	2.46	–	−4.806	–	−2.988	−2.028	−2.9028	2.1533	0.5697	1	[−1.41, 0.37]
1.71	−2.591	−2.131	−1.198	0.557	–	0.6706	2.8896	0.6387	1	[−2.15, −0.04]	2.47	–	−4.829	–	−3.019	−2.055	−2.9339	2.1608	0.5794	1	[−1.41, 0.37]
1.72	−2.649	−2.193	−1.258	0.481	1.895	0.6564	3.0018	0.6839	0.9996	[−2.15, 0.37]	2.48	–	−4.851	–	−3.050	−2.082	−2.9647	2.1678	0.5887	1	[−1.41, 0.37]

PASA, 30, e011 (2013)
doi:10.1017/pasa.2012.011

Table 10. Continued.

Cluster →	M92	M13	M71	M67	NGC 6791						Cluster →	M92	M13	M71	M67	NGC 6791					
$(V-J)_0$	M_J					c_0	c_1	c_2	R^2	[Fe/H] Int.	$(V-J)_0$	M_J					c_0	c_1	c_2	R^2	[Fe/H] Int.
1.73	−2.706	−2.253	−1.316	0.406	1.784	0.5706	2.9565	0.6684	0.9997	[−2.15, 0.37]	2.49	–	−4.873	–	−3.081	−2.109	−2.9950	2.1743	0.5975	1	[−1.41, 0.37]
1.74	−2.762	−2.312	−1.374	0.333	1.676	0.4867	2.9127	0.6533	0.9998	[−2.15, 0.37]	2.50	–	−4.895	–	−3.111	−2.135	−3.0250	2.1804	0.6059	1	[−1.41, 0.37]
1.75	−2.817	−2.370	−1.431	0.261	1.571	0.4047	2.8703	0.6387	0.9999	[−2.15, 0.37]	2.51	–	−4.916	–	−3.141	−2.162	−3.0546	2.1859	0.6139	1	[−1.41, 0.37]
1.76	−2.872	−2.427	−1.487	0.190	1.468	0.3245	2.8291	0.6245	0.9999	[−2.15, 0.37]	2.52	–	−4.937	–	−3.170	−2.188	−3.0837	2.1908	0.6213	1	[−1.41, 0.37]
1.77	−2.926	−2.483	−1.541	0.121	1.368	0.2461	2.7893	0.6107	1	[−2.15, 0.37]	2.53	–	−4.958	–	−3.199	−2.214	−3.1123	2.1951	0.6282	1	[−1.41, 0.37]
1.78	−2.979	−2.537	−1.595	0.053	1.271	0.1695	2.7507	0.5973	1	[−2.15, 0.37]	2.54	–	−4.979	–	−3.227	−2.240	−3.1405	2.1987	0.6346	1	[−1.41, 0.37]
1.79	−3.032	−2.591	−1.648	−0.014	1.176	0.0945	2.7133	0.5842	0.9999	[−2.15, 0.37]	2.55	–	−5.000	–	−3.255	−2.266	−3.1683	2.2017	0.6404	1	[−1.41, 0.37]
1.80	−3.084	−2.643	−1.700	−0.080	1.083	0.0213	2.6771	0.5715	0.9999	[−2.15, 0.37]	2.56	–	−5.020	–	−3.283	−2.292	−3.1955	2.2039	0.6455	1	[−1.41, 0.37]
1.81	−3.135	−2.694	−1.752	−0.144	0.993	−0.0504	2.6420	0.5591	0.9999	[−2.15, 0.37]	2.57	–	−5.040	–	−3.309	−2.317	−3.2222	2.2054	0.6500	1	[−1.41, 0.37]
1.82	−3.186	−2.745	−1.802	−0.208	0.905	−0.1204	2.6080	0.5470	0.9998	[−2.15, 0.37]	2.58	–	−5.059	–	−3.336	−2.343	−3.2484	2.2061	0.6539	1	[−1.41, 0.37]
1.83	−3.237	−2.794	−1.851	−0.270	0.819	−0.1890	2.5750	0.5353	0.9998	[−2.15, 0.37]	2.59	–	−5.078	–	−3.361	−2.368	−3.2740	2.2060	0.6570	1	[−1.41, 0.37]
1.84	−3.286	−2.843	−1.900	−0.331	0.736	−0.2560	2.5431	0.5238	0.9997	[−2.15, 0.37]	2.60	–	−5.097	–	−3.386	−2.393	−3.2990	2.2051	0.6594	1	[−1.41, 0.37]
1.85	−3.336	−2.890	−1.948	−0.391	0.655	−0.3215	2.5122	0.5126	0.9996	[−2.15, 0.37]	2.61	–	−5.116	–	−3.411	−2.418	−3.3235	2.2032	0.6611	1	[−1.41, 0.37]
1.86	−3.385	−2.937	−1.995	−0.450	0.576	−0.3856	2.4822	0.5017	0.9996	[−2.15, 0.37]	2.62	–	−5.134	–	−3.434	−2.443	−3.3473	2.2004	0.6620	1	[−1.41, 0.37]
1.87	−3.433	−2.982	−2.041	−0.509	0.498	−0.4484	2.4532	0.4910	0.9995	[−2.15, 0.37]	2.63	–	−5.152	–	−3.457	−2.467	−3.3705	2.1967	0.6621	1	[−1.41, 0.37]
1.88	−3.481	−3.027	−2.086	−0.566	0.423	−0.5097	2.4251	0.4806	0.9994	[−2.15, 0.37]	2.64	–	−5.169	–	−3.480	−2.492	−3.3931	2.1920	0.6613	1	[−1.41, 0.37]
1.89	−3.529	−3.071	−2.131	−0.622	0.350	−0.5698	2.3978	0.4704	0.9994	[−2.15, 0.37]	2.65	–	−5.186	–	−3.501	−2.516	−3.4149	2.1862	0.6597	1	[−1.41, 0.37]
1.90	−3.576	−3.114	−2.175	−0.678	0.278	−0.6286	2.3713	0.4604	0.9993	[−2.15, 0.37]	2.66	–	−5.203	–	−3.522	−2.540	−3.4361	2.1794	0.6572	1	[−1.41, 0.37]
1.91	−3.623	−3.157	−2.218	−0.733	0.209	−0.6861	2.3457	0.4507	0.9992	[−2.15, 0.37]	2.67	–	−5.219	–	−3.542	−2.564	−3.4565	2.1716	0.6537	1	[−1.41, 0.37]
1.92	−3.669	−3.199	−2.260	−0.786	0.141	−0.7425	2.3209	0.4412	0.9992	[−2.15, 0.37]	2.68	–	−5.234	–	−3.562	−2.587	−3.4761	2.1626	0.6494	1	[−1.41, 0.37]
1.93	−3.715	−3.240	−2.302	−0.840	0.075	−0.7977	2.2968	0.4318	0.9991	[−2.15, 0.37]	2.69	–	–	–	−3.580	−2.610	2.3650	−3.4855	–	1	[−0.04, 0.37]
1.94	−3.761	−3.280	−2.343	−0.892	0.010	−0.8517	2.2735	0.4227	0.9991	[−2.15, 0.37]	2.70	–	–	–	−3.598	−2.634	2.3515	−3.5036	–	1	[−0.04, 0.37]
1.95	−3.806	−3.320	−2.383	−0.944	−0.053	−0.9047	2.2509	0.4138	0.9991	[−2.15, 0.37]	2.71	–	–	–	−3.614	−2.656	2.3366	−3.5209	–	1	[−0.04, 0.37]
1.96	−3.851	−3.359	−2.422	−0.994	−0.114	−0.9565	2.2289	0.4051	0.9990	[−2.15, 0.37]	2.72	–	–	–	−3.630	−2.679	2.3200	−3.5374	–	1	[−0.04, 0.37]
1.97	−3.895	−3.397	−2.461	−1.045	−0.174	−1.0074	2.2077	0.3966	0.9990	[−2.15, 0.37]	2.73	–	–	–	−3.645	−2.701	2.3018	−3.5529	–	1	[−0.04, 0.37]
1.98	−3.939	−3.435	−2.499	−1.094	−0.232	−1.0572	2.1871	0.3882	0.9990	[−2.15, 0.37]	2.74	–	–	–	−3.659	−2.723	2.2820	−3.5676	–	1	[−0.04, 0.37]
1.99	−3.983	−3.472	−2.537	−1.143	−0.289	−1.1061	2.1671	0.3801	0.9990	[−2.15, 0.37]	2.75	–	–	–	−3.672	−2.745	2.2604	−3.5813	–	1	[−0.04, 0.37]
2.00	−4.026	−3.509	−2.574	−1.192	−0.345	−1.1541	2.1478	0.3721	0.9990	[−2.15, 0.37]	2.76	–	–	–	−3.683	−2.766	2.2371	−3.5940	–	1	[−0.04, 0.37]
2.01	−4.069	−3.545	−2.610	−1.239	−0.399	−1.2011	2.1290	0.3644	0.9990	[−2.15, 0.37]	2.77	–	–	–	−3.694	−2.787	2.2120	−3.6057	–	1	[−0.04, 0.37]
2.02	−4.111	−3.580	−2.646	−1.287	−0.452	−1.2473	2.1109	0.3568	0.9990	[−2.15, 0.37]	2.78	–	–	–	−3.704	−2.808	2.1851	−3.6164	–	1	[−0.04, 0.37]
2.03	−4.153	−3.615	−2.681	−1.333	−0.504	−1.2926	2.0933	0.3494	0.9991	[−2.15, 0.37]	2.79	–	–	–	−3.712	−2.828	2.1564	−3.6260	–	1	[−0.04, 0.37]
2.04	−4.194	−3.650	−2.716	−1.379	−0.554	−1.3371	2.0762	0.3423	0.9991	[−2.15, 0.37]	2.80	–	–	–	−3.719	−2.848	2.1257	−3.6344	–	1	[−0.04, 0.37]
2.05	−4.235	−3.684	−2.750	−1.425	−0.604	−1.3809	2.0598	0.3353	0.9991	[−2.15, 0.37]	–	–	–	–	–	–	–	–	–	–	–

Note. The 11th and 22nd columns give the range of the metallicity [Fe/H] (dex) for the star whose absolute magnitude would be estimated. R^2 is the square of the correlation coefficient.

Table 11. M_{K_s} Absolute Magnitudes Estimated for a Set of $(V-K_s)_0$ Colours for Five Clusters used in the Calibration

Cluster→	M92	M13	M71	M67	NGC 6791
$(V-K_s)_0$			M_{K_s}		
1.75	0.957	1.456	–	–	–
1.80	0.434	0.919	1.742	–	–
1.85	– 0.045	0.424	1.250	–	–
1.90	– 0.485	– 0.031	0.792	–	–
1.95	– 0.890	– 0.449	0.367	–	–
2.00	– 1.265	– 0.834	– 0.028	–	–
2.05	– 1.613	– 1.189	– 0.394	–	–
2.10	– 1.938	– 1.515	– 0.733	–	–
2.15	– 2.242	– 1.816	– 1.048	0.960	–
2.20	– 2.529	– 2.094	– 1.339	0.635	–
2.25	– 2.800	– 2.352	– 1.608	0.320	–
2.30	– 3.059	– 2.591	– 1.857	0.016	–
2.35	– 3.306	– 2.814	– 2.088	– 0.274	–
2.40	– 3.543	– 3.023	– 2.302	– 0.550	–
2.45	– 3.771	– 3.219	– 2.500	– 0.811	0.619
2.50	– 3.992	– 3.403	– 2.683	– 1.057	0.256
2.55	– 4.204	– 3.578	– 2.854	– 1.288	– 0.072
2.60	– 4.408	– 3.745	– 3.012	– 1.505	– 0.369
2.65	– 4.605	– 3.905	– 3.160	– 1.709	– 0.637
2.70	– 4.793	– 4.058	– 3.299	– 1.901	– 0.880
2.75	– 4.971	– 4.206	– 3.428	– 2.083	– 1.101
2.80	– 5.138	– 4.350	– 3.550	– 2.255	– 1.302
2.85	– 5.292	– 4.490	– 3.666	– 2.421	– 1.486
2.90	– 5.432	– 4.626	– 3.776	– 2.581	– 1.656
2.95	– 5.556	– 4.759	– 3.881	– 2.736	– 1.813
3.00	– 5.659	– 4.890	– 3.981	– 2.890	– 1.960
3.05	– 5.740	– 5.017	– 4.078	– 3.042	– 2.098
3.10	–	– 5.142	– 4.172	– 3.194	– 2.230
3.15	–	– 5.264		– 3.347	– 2.357
3.20	–	– 5.381	–	– 3.501	– 2.479
3.30	–	– 5.604	–	– 3.815	– 2.717
3.35	–	– 5.708	–	– 3.973	– 2.834
3.40	–	– 5.805	–	– 4.130	– 2.951
3.45	–	– 5.894	–	– 4.285	– 3.067
3.50	–	– 5.975	–	– 4.435	– 3.184
3.55	–	– 6.045	–	– 4.576	– 3.301
3.60	–	– 6.104	–	– 4.705	– 3.418
3.65	–	– 6.149	–	– 4.817	– 3.535
3.70	–	– 6.179	–	– 4.905	– 3.651
3.75	–	–	–	– 4.963	– 3.766
3.80	–	–	–	– 4.984	– 3.878
3.85	–	–	–	–	– 3.988
3.90	–	–	–	–	– 4.092
3.95	–	–	–	–	– 4.191
4.00	–	–	–	–	– 4.283
4.05	–	–	–	–	– 4.365
4.10	–	–	–	–	– 4.436

Iron abundance, [Fe/H], is not the only parameter that determines the chemistry of the star, but α enhancement, $[\alpha/\mathrm{Fe}]$, is also equally important. However, as stated in Paper I, there is a correlation between the two sets of abundances. Hence, we do not expect any considerable change in the numerical values of the estimated absolute magnitudes in the case of addition of the α-enhancement term in Equations (7) and (9).

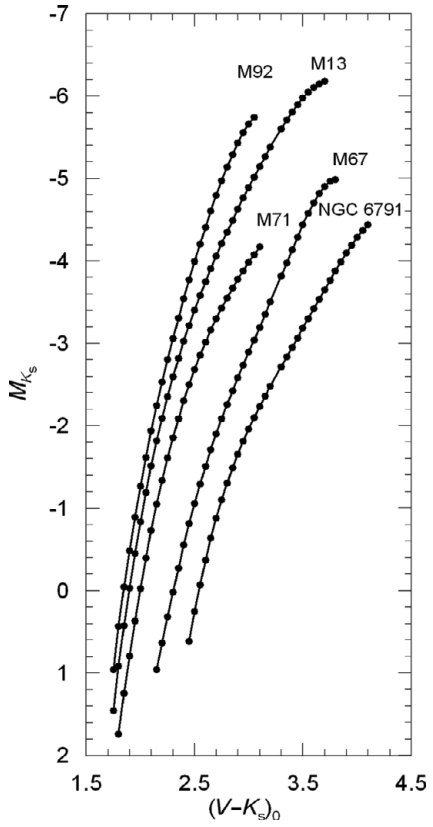

Figure 5. $M_{K_s} \times (V-K_s)_0$ colour–absolute magnitude diagrams for five clusters used for the absolute magnitude calibration.

3.2 Application of the Method

3.2.1 Application of the $M_J \times$ [Fe/H] Calibration

We applied the $M_J \times$ [Fe/H] calibration to the clusters M5 and M68. The reason for choosing clusters instead of field giants is that clusters provide absolute magnitudes for comparison with the ones estimated by means of our method. The J magnitudes and $V-J$ colours for the cluster M5 are taken from Brasseur et al. (2010). 2MASS photometric data are not available for the cluster M68. Hence, the J_0 magnitudes and $(V-J)_0$ colours are provided by transformation of the V, $B-V$, and $V-I$ data of Walker (1994) to J_0 magnitudes and $(V-J)_0$ colours by Equation (1) and the procedure explained in Section 2.1. The data for the clusters are given in Table 14. Two references are given for the cluster M5. The colour excess $E(B-V)$ and the true distance modulus μ_0 refer to the first author, whereas the metallicity which was tested in Paper I is taken from the second author. The J_0 magnitudes and $(V-J)_0$ colours as well as the original V, $B-V$, and $V-I$ data are given in Table 15.

We evaluated the M_J absolute magnitude by Equation (7) for a set of $(V-J)_0$ colour indices where the clusters are defined. The results are given in Table 16. The columns refer to (1) $(V-J)_0$ colour index; (2) $(M_J)_{\mathrm{cl}}$, the absolute magnitude for a cluster estimated by its colour–magnitude diagram; (3) $(M_J)_{\mathrm{ev}}$, the absolute magnitude estimated by the procedure;

Table 12. M_{K_s} Absolute Magnitudes and [Fe/H] Metallicities for Seven $(V-K_s)_0$ Intervals

$(V-K_s)_0$	[Fe/H] (dex)	M_{K_s}
1.80	−2.15	0.434
	−1.41	0.919
	−0.78	1.742
2.00	−2.15	−1.265
	−1.41	−0.834
	−0.78	−0.028
2.20	−2.15	−2.529
	−1.41	−2.094
	−0.78	−1.339
	−0.04	0.635
2.40	−2.15	−3.543
	−1.41	−3.023
	−0.78	−2.302
	−0.04	−0.550
2.60	−2.15	−4.408
	−1.41	−3.745
	−0.78	−3.012
	−0.04	−1.505
	0.37	−0.369
3.00	−2.15	−5.659
	−1.41	−4.890
	−0.78	−3.981
	−0.04	−2.890
	0.37	−1.960
3.30	−1.41	−5.604
	−0.04	−3.815
	0.37	−2.717

(4) ΔM_J, absolute magnitude residuals. Also, the metallicity for each cluster is indicated near the name of the cluster. The differences between the absolute magnitudes estimated by the procedure presented in this study and those evaluated via colour–magnitude diagrams of the clusters (the residuals) lie in a (relatively) short interval, i.e. −0.08 and +0.34 mag, and the range of 94% of the absolute magnitude residuals is only $0 < M_J \leq 0.3$ mag. The mean and the standard deviation of (all) residuals are $\langle \Delta M_J \rangle = 0.137$ and $\sigma_{M_J} = 0.080$ mag, respectively. The distribution of the residuals are given in Table 17 and Figure 7.

3.2.2 Application of the M_{K_s} × [Fe/H] Calibration

NGC 1851 is the last cluster in Brasseur et al. (2010) for which K_s magnitudes and $V-K_s$ colours are available. However, the $M_{K_s} \times (V-K_s)_0$ colour–magnitude diagram of this cluster shows that the uncertainties in the data of this cluster are (relatively) large. Actually, the absolute magnitudes are fainter than the corresponding ones of the cluster M71 for the colour interval $(V-K_s)_0 < 2.5$ mag but brighter for $(V-K_s)_0 > 2.5$ mag. This trend holds for distance modulus and colour excess in Brasseur et al. (2010), i.e. $\mu = 15.50$ and $E(B-V) = 0.034$ mag, as well as for alternative data such as $E(B-V) = 0.02$ and $\mu_0 = 15.50 \pm 0.20$ mag of Saviane et al. (1998). If we regard the metallicity claimed by Brasseur et al. (2010), [Fe/H] = −1.40 dex, the absolute magnitude colour diagram of the cluster NGC 1851 should coincide with that of M13 ([Fe/H] = −1.41 dex). The alternative metallicity of Rosenberg et al. (1999), [Fe/H] $= -1.03 \pm 0.06$ dex, should replace the absolute magnitude colour diagram of NGC 1851 between the diagrams of M13 and M71, which is not the case. $M_{K_s} \times (V-K_s)_0$ diagrams for three clusters mentioned in this paragraph are not plotted because of space constraints.

Then, we transformed the V, $B-V$, and $V-I$ data of NGC 188 (Stetson et al. 2004) and M68 (Walker 1994) to the K_{s_0} magnitudes and $(V-K_s)_0$ colours by Equation (3) and the procedure explained in Section 2.2. Colour excess $E(B-V)$, distance modulus μ_0, and metallicity for the clusters are given in Table 14. The second reference for the cluster NGC 188 is given for the metallicity only, whereas the first

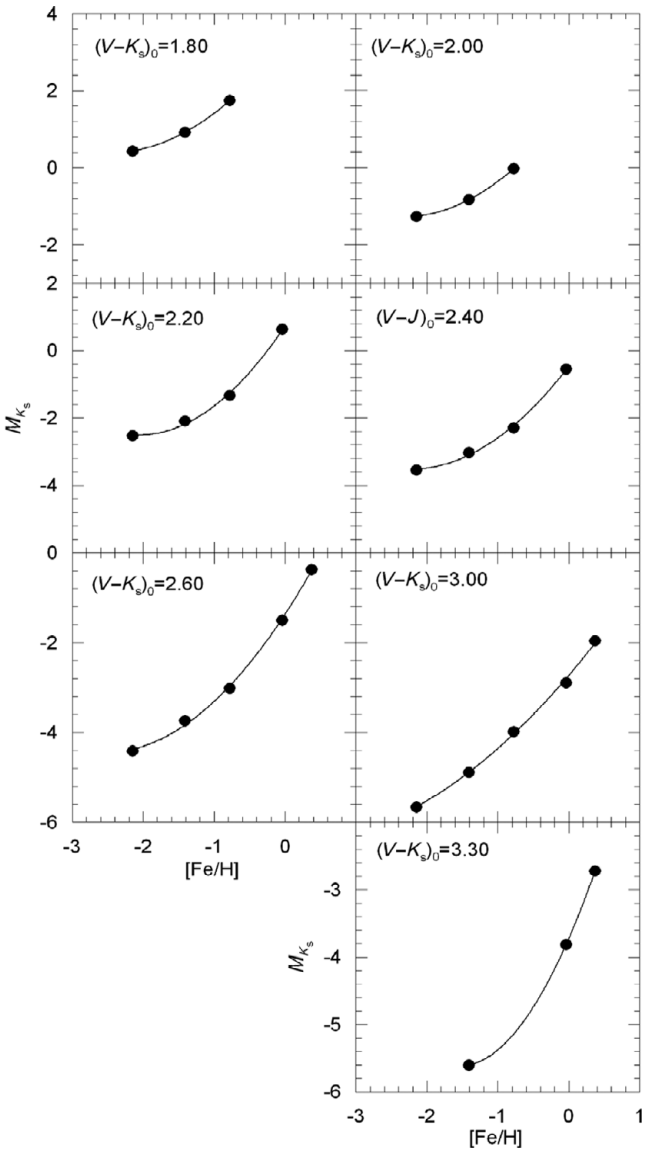

Figure 6. Calibration of the absolute magnitude M_{K_s} as a function of metallicity [Fe/H] for seven colour indices.

https://doi.org/10.1017/pasa.2012.011 Published online by Cambridge University Press

PASA, 30, e011 (2013)
doi:10.1017/pasa.2012.011

Table 13. M_{K_s} Absolute Magnitudes Estimated for Five Galactic Clusters and the Numerical Values of d_i ($i = 0, 1, 2$) Coefficients in Equation (9)

Cluster→	M92	M13	M71	M67	NGC 6791						Cluster→	M92	M13	M71	M67	NGC 6791					
$(V-K_s)_0$	M_{K_s}					d_0	d_1	d_2	R^2	[Fe/H] Int.	$(V-K_s)_0$	M_{K_s}					d_0	d_1	d_2	R^2	[Fe/H] Int.
1.75	0.957	1.456	–	–	–	2.4069	0.6743	–	1	[−2.15, −1.41]	2.78	−5.072	−4.293	−3.502	−2.187	−1.224	−2.0618	2.0624	0.3127	0.9993	[−2.15, 0.37]
1.76	0.849	1.345	–	–	–	2.2905	0.6705	–	1	[−2.15, −1.41]	2.79	−5.105	−4.322	−3.527	−2.222	−1.263	−2.0954	2.0480	0.3060	0.9993	[−2.15, 0.37]
1.77	0.742	1.236	–	–	–	2.1757	0.6667	–	1	[−2.15, −1.41]	2.80	−5.138	−4.350	−3.550	−2.255	−1.302	−2.1286	2.0342	0.2996	0.9993	[−2.15, 0.37]
1.78	0.638	1.128	–	–	–	2.0626	0.6627	–	1	[−2.15, −1.41]	2.81	−5.170	−4.378	−3.574	−2.289	−1.340	−2.1613	2.0209	0.2935	0.9993	[−2.15, 0.37]
1.79	0.535	1.023	1.845	–	–	3.3824	2.3393	0.4721	1	[−2.15, −0.78]	2.82	−5.201	−4.406	−3.597	−2.322	−1.377	−2.1937	2.0081	0.2876	0.9993	[−2.15, 0.37]
1.80	0.434	0.919	1.742	–	–	3.2861	2.3511	0.4766	1	[−2.15, −0.78]	2.83	−5.232	−4.434	−3.621	−2.355	−1.414	−2.2256	1.9957	0.2819	0.9993	[−2.15, 0.37]
1.81	0.335	0.816	1.641	–	–	3.1907	2.3618	0.4807	1	[−2.15, −0.78]	2.84	−5.263	−4.462	−3.643	−2.388	−1.450	−2.2572	1.9839	0.2766	0.9994	[−2.15, 0.37]
1.82	0.238	0.716	1.541	–	–	3.0961	2.3716	0.4847	1	[−2.15, −0.78]	2.85	−5.292	−4.490	−3.666	−2.421	−1.486	−2.2885	1.9725	0.2715	0.9994	[−2.15, 0.37]
1.83	0.142	0.617	1.443	–	–	3.0023	2.3804	0.4883	1	[−2.15, −0.78]	2.86	−5.322	−4.517	−3.688	−2.453	−1.521	−2.3194	1.9616	0.2666	0.9993	[−2.15, 0.37]
1.84	0.048	0.520	1.346	–	–	2.9094	2.3882	0.4917	1	[−2.15, −0.78]	2.87	−5.350	−4.545	−3.711	−2.485	−1.555	−2.3501	1.9512	0.2621	0.9993	[−2.15, 0.37]
1.85	−0.045	0.424	1.250	–	–	2.8172	2.3951	0.4948	1	[−2.15, −0.78]	2.88	−5.378	−4.572	−3.733	−2.517	−1.589	−2.3804	1.9413	0.2578	0.9993	[−2.15, 0.37]
1.86	−0.136	0.330	1.156	–	–	2.7259	2.4011	0.4976	1	[−2.15, −0.78]	2.89	−5.406	−4.599	−3.754	−2.549	−1.623	−2.4104	1.9318	0.2538	0.9993	[−2.15, 0.37]
1.87	−0.225	0.237	1.063	–	–	2.6355	2.4061	0.5002	1	[−2.15, −0.78]	2.90	−5.432	−4.626	−3.776	−2.581	−1.656	−2.4402	1.9227	0.2501	0.9993	[−2.15, 0.37]
1.88	−0.313	0.146	0.972	–	–	2.5458	2.4103	0.5025	1	[−2.15, −0.78]	2.91	−5.459	−4.653	−3.797	−2.612	−1.688	−2.4697	1.9142	0.2467	0.9992	[−2.15, 0.37]
1.89	−0.400	0.057	0.881	–	–	2.4570	2.4136	0.5046	1	[−2.15, −0.78]	2.92	−5.484	−4.680	−3.818	−2.643	−1.720	−2.4989	1.9060	0.2436	0.9992	[−2.15, 0.37]
1.90	−0.485	−0.031	0.792	–	–	2.3689	2.4161	0.5064	1	[−2.15, −0.78]	2.93	−5.509	−4.706	−3.839	−2.675	−1.751	−2.5280	1.8983	0.2409	0.9991	[−2.15, 0.37]
1.91	−0.569	−0.118	0.705	–	–	2.2817	2.4177	0.5079	1	[−2.15, −0.78]	2.94	−5.532	−4.733	−3.860	−2.706	−1.782	−2.5568	1.8911	0.2384	0.9991	[−2.15, 0.37]
1.92	−0.651	−0.203	0.619	–	–	2.1952	2.4184	0.5091	1	[−2.15, −0.78]	2.95	−5.556	−4.759	−3.881	−2.736	−1.813	−2.5854	1.8842	0.2362	0.9990	[−2.15, 0.37]
1.93	−0.732	−0.286	0.534	–	–	2.1096	2.4184	0.5101	1	[−2.15, −0.78]	2.96	−5.578	−4.786	−3.901	−2.767	−1.843	−2.6138	1.8779	0.2344	0.9989	[−2.15, 0.37]
1.94	−0.812	−0.369	0.450	–	–	2.0247	2.4176	0.5108	1	[−2.15, −0.78]	2.97	−5.600	−4.812	−3.921	−2.798	−1.873	−2.6421	1.8719	0.2329	0.9989	[−2.15, 0.37]
1.95	−0.890	−0.449	0.367	–	–	1.9406	2.4160	0.5113	1	[−2.15, −0.78]	2.98	−5.620	−4.838	−3.941	−2.829	−1.902	−2.6707	1.8664	0.2317	0.9988	[−2.15, 0.37]
1.96	−0.968	−0.529	0.286	–	–	1.8573	2.4137	0.5115	1	[−2.15, −0.78]	2.99	−5.640	−4.864	−3.961	−2.859	−1.931	−2.6982	1.8613	0.2309	0.9986	[−2.15, 0.37]
1.97	−1.044	−0.607	0.206	–	–	1.7748	2.4106	0.5115	1	[−2.15, −0.78]	3.00	−5.659	−4.890	−3.981	−2.890	−1.960	−2.7260	1.8566	0.2304	0.9985	[−2.15, 0.37]
1.98	−1.119	−0.684	0.127	–	–	1.6931	2.4068	0.5112	1	[−2.15, −0.78]	3.01	−5.677	−4.916	−4.001	−2.920	−1.988	−2.7537	1.8524	0.2303	0.9984	[−2.15, 0.37]
1.99	−1.192	−0.760	0.049	–	–	1.6112	2.4023	0.5106	1	[−2.15, −0.78]	3.02	−5.695	−4.941	−4.020	−2.951	−2.016	−2.7813	1.8485	0.2303	0.9982	[−2.15, 0.37]
2.00	−1.265	−0.834	−0.028	–	–	1.5320	2.3972	0.5098	1	[−2.15, −0.78]	3.03	−5.711	−4.967	−4.040	−2.981	−2.044	−2.8088	1.8451	0.2312	0.9980	[−2.15, 0.37]
2.01	−1.337	−0.908	−0.103	–	–	1.4526	2.3913	0.5088	1	[−2.15, −0.78]	3.04	−5.726	−4.992	−4.059	−3.011	−2.071	−2.8362	1.8421	0.2322	0.9978	[−2.15, 0.37]
2.02	−1.407	−0.980	−0.177	–	–	1.3740	2.3848	0.5075	1	[−2.15, −0.78]	3.05	–	−5.017	−4.078	−3.042	−2.098	−2.8651	1.8452	0.2401	0.9957	[−1.41, 0.37]
2.03	−1.477	−1.050	−0.251	–	–	1.2961	2.3777	0.5060	1	[−2.15, −0.78]	3.06	–	−5.043	−4.097	−3.072	−2.125	−2.8910	1.8379	0.2359	0.9953	[−1.41, 0.37]
2.04	−1.546	−1.120	−0.323	–	–	1.2191	2.3700	0.5042	1	[−2.15, −0.78]	3.07	–	−5.068	−4.116	−3.103	−2.152	−2.9168	1.8307	0.2319	0.9949	[−1.41, 0.37]
2.05	−1.613	−1.189	−0.394	–	–	1.1427	2.3617	0.5022	1	[−2.15, −0.78]	3.08	–	−5.093	−4.135	−3.133	−2.178	−2.9426	1.8238	0.2281	0.9944	[−1.41, 0.37]
2.06	−1.680	−1.256	−0.464	–	–	1.0672	2.3528	0.5000	1	[−2.15, −0.78]	3.09	–	−5.117	−4.154	−3.163	−2.204	−2.9682	1.8171	0.2244	0.9939	[−1.41, 0.37]
2.07	−1.746	−1.322	−0.533	–	–	0.9924	2.3433	0.4976	1	[−2.15, −0.78]	3.10	–	−5.142	−4.172	−3.194	−2.230	−2.9938	1.8106	0.2210	0.9933	[−1.41, 0.37]
2.08	−1.811	−1.388	−0.601	–	–	0.9184	2.3333	0.4949	1	[−2.15, −0.78]	3.11	–	−5.167	–	−3.224	−2.256	−3.1378	2.1872	0.5307	1	[−1.41, 0.37]
2.09	−1.875	−1.452	−0.667	–	–	0.8451	2.3228	0.4920	1	[−2.15, −0.78]	3.12	–	−5.191	–	−3.255	−2.281	−3.1680	2.1964	0.5401	1	[−1.41, 0.37]
2.10	−1.938	−1.515	−0.733	–	–	0.7726	2.3118	0.4889	1	[−2.15, −0.78]	3.13	–	−5.215	–	−3.286	−2.307	−3.1982	2.2061	0.5500	1	[−1.41, 0.37]
2.11	−2.000	−1.577	−0.798	–	–	0.7008	2.3003	0.4856	1	[−2.15, −0.78]	3.14	–	−5.240	–	−3.316	−2.332	−3.2285	2.2162	0.5602	1	[−1.41, 0.37]
2.12	−2.062	−1.638	−0.862	–	–	0.6298	2.2884	0.4821	1	[−2.15, −0.78]	3.15	–	−5.264	–	−3.347	−2.357	−3.2588	2.2266	0.5708	1	[−1.41, 0.37]
2.13	−2.123	−1.699	−0.925	–	–	0.5595	2.2760	0.4784	1	[−2.15, −0.78]	3.16	–	−5.287	–	−3.378	−2.382	−3.2891	2.2375	0.5818	1	[−1.41, 0.37]
2.14	−2.183	−1.758	−0.987	–	–	0.4900	2.2632	0.4744	1	[−2.15, −0.78]	3.17	–	−5.311	–	−3.408	−2.406	−3.3195	2.2488	0.5931	1	[−1.41, 0.37]
2.15	−2.242	−1.816	−1.048	0.960	–	1.0614	3.202	0.7802	0.9973	[−2.15, −0.04]	3.18	–	−5.335	–	−3.439	−2.431	−3.3499	2.2605	0.6048	1	[−1.41, 0.37]
2.16	−2.301	−1.874	−1.108	0.895	–	0.9953	3.1913	0.7768	0.9973	[−2.15, −0.04]	3.19	–	−5.358	–	−3.470	−2.455	−3.3804	2.2725	0.6169	1	[−1.41, 0.37]

PASA, 30, e011 (2013)
doi:10.1017/pasa.2012.011

Table 13. Continued.

Cluster→	M92	M13	M71	M67	NGC 6791						Cluster→	M92	M13	M71	M67	NGC 6791					
$(V-K_s)_0$	M_{K_s}					d_0	d_1	d_2	R^2	[Fe/H] Int.	$(V-K_s)_0$	M_{K_s}					d_0	d_1	d_2	R^2	[Fe/H] Int.
2.17	−2.359	−1.930	−1.167	0.829	–	0.9295	3.1795	0.7731	0.9973	[−2.15, −0.04]	3.20	–	−5.381	–	−3.501	−2.479	−3.4110	2.2848	0.6293	1	[−1.41, 0.37]
2.18	−2.416	−1.986	−1.225	0.764	–	0.8640	3.1667	0.7689	0.9973	[−2.15, −0.04]	3.21	–	−5.405	–	−3.532	−2.504	−3.4415	2.2975	0.6421	1	[−1.41, 0.37]
2.19	−2.473	−2.041	−1.282	0.700	–	0.7987	3.1528	0.7643	0.9972	[−2.15, −0.04]	3.22	–	−5.427	–	−3.564	−2.528	−3.4722	2.3105	0.6551	1	[−1.41, 0.37]
2.20	−2.529	−2.094	−1.339	0.635	–	0.7338	3.1381	0.7594	0.9972	[−2.15, −0.04]	3.23	–	−5.450	–	−3.595	−2.552	−3.5029	2.3237	0.6685	1	[−1.41, 0.37]
2.21	−2.584	−2.148	−1.394	0.572	–	0.6693	3.1225	0.7541	0.9972	[−2.15, −0.04]	3.24	–	−5.473	–	−3.626	−2.575	−3.5337	2.3372	0.6822	1	[−1.41, 0.37]
2.22	−2.639	−2.200	−1.449	0.508	–	0.6052	3.1062	0.7485	0.9972	[−2.15, −0.04]	3.25	–	−5.495	–	−3.657	−2.599	−3.5645	2.3510	0.6962	1	[−1.41, 0.37]
2.23	−2.694	−2.251	−1.503	0.445	–	0.5414	3.0890	0.7425	0.9972	[−2.15, −0.04]	3.26	–	−5.517	–	−3.689	−2.623	−3.5953	2.3650	0.7105	1	[−1.41, 0.37]
2.24	−2.747	−2.302	−1.556	0.382	–	0.4781	3.0712	0.7363	0.9972	[−2.15, −0.04]	3.27	–	−5.539	–	−3.720	−2.647	−3.6262	2.3792	0.7250	1	[−1.41, 0.37]
2.25	−2.800	−2.352	−1.608	0.320	–	0.4152	3.0527	0.7298	0.9972	[−2.15, −0.04]	3.28	–	−5.561	–	−3.752	−2.670	−3.6572	2.3935	0.7398	1	[−1.41, 0.37]
2.26	−2.853	−2.401	−1.660	0.258	–	0.3527	3.0337	0.7230	0.9972	[−2.15, −0.04]	3.29	–	−5.583	–	−3.783	−2.694	−3.6881	2.4080	0.7548	1	[−1.41, 0.37]
2.27	−2.905	−2.450	−1.710	0.197	–	0.2908	3.0140	0.7160	0.9972	[−2.15, −0.04]	3.30	–	−5.604	–	−3.815	−2.717	−3.7192	2.4227	0.7700	1	[−1.41, 0.37]
2.28	−2.957	−2.498	−1.760	0.136	–	0.2293	2.9939	0.7087	0.9972	[−2.15, −0.04]	3.31	–	−5.625	–	−3.846	−2.741	−3.7502	2.4374	0.7854	1	[−1.41, 0.37]
2.29	−3.008	−2.545	−1.809	0.076	–	0.1683	2.9732	0.7012	0.9972	[−2.15, −0.04]	3.32	–	−5.646	–	−3.878	−2.764	−3.7812	2.4522	0.8010	1	[−1.41, 0.37]
2.30	−3.059	−2.591	−1.857	0.016	–	0.1079	2.9522	0.6935	0.9972	[−2.15, −0.04]	3.33	–	−5.667	–	−3.910	−2.788	−3.8123	2.4671	0.8168	1	[−1.41, 0.37]
2.31	−3.109	−2.637	−1.905	−0.043	–	0.0480	2.9307	0.6856	0.9972	[−2.15, −0.04]	3.34	–	−5.688	–	−3.941	−2.811	−3.8433	2.4820	0.8327	1	[−1.41, 0.37]
2.32	−3.159	−2.683	−1.952	−0.102	–	−0.1140	2.9089	0.6774	0.9972	[−2.15, −0.04]	3.35	–	−5.708	–	−3.973	−2.834	−3.8744	2.4969	0.8487	1	[−1.41, 0.37]
2.33	−3.209	−2.727	−1.998	−0.160	–	−0.0702	2.8868	0.6692	0.9972	[−2.15, −0.04]	3.36	–	−5.728	–	−4.004	−2.858	−3.9054	2.5117	0.8647	1	[−1.41, 0.37]
2.34	−3.257	−2.771	−2.043	−0.217	–	−0.1285	2.8644	0.6607	0.9972	[−2.15, −0.04]	3.37	–	−5.747	–	−4.036	−2.881	−3.9364	2.5264	0.8809	1	[−1.41, 0.37]
2.35	−3.306	−2.814	−2.088	−0.274	–	−0.1862	2.8418	0.6521	0.9972	[−2.15, −0.04]	3.38	–	−5.767	–	−4.068	−2.904	−3.9673	2.5411	0.8971	1	[−1.41, 0.37]
2.36	−3.354	−2.857	−2.132	−0.331	–	−0.2433	2.8189	0.6434	0.9972	[−2.15, −0.04]	3.39	–	−5.786	–	−4.099	−2.928	−3.9982	2.5556	0.9133	1	[−1.41, 0.37]
2.37	−3.402	−2.900	−2.176	−0.386	–	−0.2998	2.7959	0.6345	0.9973	[−2.15, −0.04]	3.40	–	−5.805	–	−4.130	−2.951	−4.0290	2.5699	0.9294	1	[−1.41, 0.37]
2.38	−3.450	−2.941	−2.218	−0.442	–	−0.3558	2.7727	0.6255	0.9973	[−2.15, −0.04]	3.41	–	−5.823	–	−4.162	−2.974	−4.0597	2.5839	0.9455	1	[−1.41, 0.37]
2.39	−3.497	−2.982	−2.260	−0.496	–	−0.4111	2.7494	0.6164	0.9973	[−2.15, −0.04]	3.42	–	−5.841	–	−4.193	−2.997	−4.0903	2.5977	0.9616	1	[−1.41, 0.37]
2.40	−3.543	−3.023	−2.302	−0.550	–	−0.4658	2.7259	0.6072	0.9973	[−2.15, −0.04]	3.43	–	−5.859	–	−4.224	−3.021	−4.1208	2.6112	0.9775	1	[−1.41, 0.37]
2.41	−3.590	−3.063	−2.343	−0.604	–	−0.5200	2.7024	0.5980	0.9974	[−2.15, −0.04]	3.44	–	−5.877	–	−4.254	−3.044	−4.1511	2.6244	0.9932	1	[−1.41, 0.37]
2.42	−3.636	−3.103	−2.383	−0.656	–	−0.5735	2.6789	0.5886	0.9974	[−2.15, −0.04]	3.45	–	−5.894	–	−4.285	−3.067	−4.1813	2.6372	1.0088	1	[−1.41, 0.37]
2.43	−3.681	−3.142	−2.422	−0.709	–	−0.6264	2.6554	0.5792	0.9974	[−2.15, −0.04]	3.46	–	−5.911	–	−4.316	−3.091	−4.2112	2.6495	1.0241	1	[−1.41, 0.37]
2.44	−3.727	−3.181	−2.461	−0.760	–	−0.6787	2.6318	0.5697	0.9975	[−2.15, −0.04]	3.47	–	−5.927	–	−4.346	−3.114	−4.2410	2.6613	1.0392	1	[−1.41, 0.37]
2.45	−3.771	−3.219	−2.500	−0.811	0.619	−0.6056	2.8777	0.6641	0.9974	[−2.15, 0.37]	3.48	–	−5.944	–	−4.376	−3.137	−4.2706	2.6726	1.0540	1	[−1.41, 0.37]
2.46	−3.816	−3.257	−2.538	−0.862	0.544	−0.6626	2.8415	0.6495	0.9976	[−2.15, 0.37]	3.49	–	−5.959	–	−4.405	−3.161	−4.2998	2.6833	1.0684	1	[−1.41, 0.37]
2.47	−3.860	−3.294	−2.575	−0.911	0.470	−0.7186	2.8060	0.6353	0.9977	[−2.15, 0.37]	3.50	–	−5.975	–	−4.435	−3.184	−4.3288	2.6934	1.0824	1	[−1.41, 0.37]
2.48	−3.904	−3.331	−2.611	−0.961	0.397	−0.7736	2.7714	0.6213	0.9978	[−2.15, 0.37]	3.51	–	−5.990	–	−4.464	−3.207	−4.3575	2.7028	1.0960	1	[−1.41, 0.37]
2.49	−3.948	−3.367	−2.648	−1.009	0.326	−0.8278	2.7377	0.6076	0.9979	[−2.15, 0.37]	3.52	–	−6.004	–	−4.493	−3.231	−4.3859	2.7114	1.1091	1	[−1.41, 0.37]
2.50	−3.992	−3.403	−2.683	−1.057	0.256	−0.8810	2.7047	0.5941	0.9980	[−2.15, 0.37]	3.53	–	−6.018	–	−4.521	−3.254	−4.4139	2.7192	1.1216	1	[−1.41, 0.37]
2.51	−4.035	−3.439	−2.718	−1.104	0.188	−0.9332	2.6725	0.5809	0.9981	[−2.15, 0.37]	3.54	–	−6.032	–	−4.549	−3.278	−4.4415	2.7262	1.1336	1	[−1.41, 0.37]
2.52	−4.077	−3.475	−2.753	−1.151	0.121	−0.9846	2.6411	0.5679	0.9982	[−2.15, 0.37]	3.55	–	−6.045	–	−4.576	−3.301	−4.4687	2.7322	1.1449	1	[−1.41, 0.37]

https://doi.org/10.1017/pasa.2012.011 Published online by Cambridge University Press

PASA, 30, e011 (2013)
doi:10.1017/pasa.2012.011

Table 13. Continued.

Cluster→	M92	M13	M71	M67	NGC 6791						Cluster→	M92	M13	M71	M67	NGC 6791					
$(V-K_s)_0$	M_{K_s}					d_0	d_1	d_2	R^2	[Fe/H] Int.	$(V-K_s)_0$	M_{K_s}					d_0	d_1	d_2	R^2	[Fe/H] Int.
2.53	−4.120	−3.510	−2.787	−1.198	0.055	−1.0351	2.6105	0.5552	0.9982	[−2.15, 0.37]	3.56	–	−6.058	–	−4.603	−3.324	−4.4954	2.7373	1.1555	1	[−1.41, 0.37]
2.54	−4.162	−3.544	−2.821	−1.243	−0.009	−1.0848	2.5806	0.5427	0.9983	[−2.15, 0.37]	3.57	–	−6.070	–	−4.629	−3.348	−4.5217	2.7412	1.1654	1	[−1.41, 0.37]
2.55	−4.204	−3.578	−2.854	−1.288	−0.072	−1.1336	2.5515	0.5303	0.9984	[−2.15, 0.37]	3.58	–	−6.082	–	−4.655	−3.371	−4.5474	2.7441	1.1745	1	[−1.41, 0.37]
2.56	−4.245	−3.612	−2.886	−1.333	−0.134	−1.1816	2.5231	0.5184	0.9984	[−2.15, 0.37]	3.59	–	−6.093	–	−4.680	−3.395	−4.5725	2.7458	1.1826	1	[−1.41, 0.37]
2.57	−4.287	−3.646	−2.919	−1.377	−0.195	−1.2287	2.4954	0.5067	0.9985	[−2.15, 0.37]	3.60	–	−6.104	–	−4.705	−3.418	−4.5971	2.7462	1.1899	1	[−1.41, 0.37]
2.58	−4.327	−3.679	−2.950	−1.420	−0.254	−1.2751	2.4684	0.4951	0.9986	[−2.15, 0.37]	3.61	–	−6.114	–	−4.729	−3.441	−4.6210	2.7452	1.1961	1	[−1.41, 0.37]
2.59	−4.368	−3.712	−2.981	−1.463	−0.312	−1.3207	2.4422	0.4838	0.9986	[−2.15, 0.37]	3.62	–	−6.123	–	−4.752	−3.465	−4.6442	2.7429	1.2013	1	[−1.41, 0.37]
2.60	−4.408	−3.745	−3.012	−1.505	−0.369	−1.3656	2.4166	0.4728	0.9987	[−2.15, 0.37]	3.63	–	−6.132	–	−4.774	−3.488	−4.6667	2.7391	1.2053	1	[−1.41, 0.37]
2.61	−4.448	−3.778	−3.043	−1.547	−0.425	−1.4096	2.3917	0.4619	0.9987	[−2.15, 0.37]	3.64	–	−6.141	–	−4.796	−3.512	−4.6885	2.7337	1.2082	1	[−1.41, 0.37]
2.62	−4.488	−3.810	−3.073	−1.588	−0.479	−1.4530	2.3675	0.4513	0.9988	[−2.15, 0.37]	3.65	–	−6.149	–	−4.817	−3.535	−4.7094	2.7266	1.2097	1	[−1.41, 0.37]
2.63	−4.527	−3.842	−3.102	−1.629	−0.533	−1.4957	2.3439	0.4409	0.9988	[−2.15, 0.37]	3.66	–	−6.156	–	−4.836	−3.558	−4.7295	2.7178	1.2099	1	[−1.41, 0.37]
2.64	−4.566	−3.873	−3.131	−1.669	−0.586	−1.5376	2.3209	0.4307	0.9988	[−2.15, 0.37]	3.67	–	−6.163	–	−4.855	−3.582	−4.7486	2.7072	1.2087	1	[−1.41, 0.37]
2.65	−4.605	−3.905	−3.160	−1.709	−0.637	−1.5789	2.2986	0.4208	0.9989	[−2.15, 0.37]	3.68	–	−6.169	–	−4.873	−3.605	−4.7669	2.6947	1.2060	1	[−1.41, 0.37]
2.66	−4.643	−3.936	−3.189	−1.748	−0.688	−1.6195	2.2770	0.4111	0.9989	[−2.15, 0.37]	3.69	–	−6.174	–	−4.889	−3.628	−4.7841	2.6802	1.2016	1	[−1.41, 0.37]
2.67	−4.681	−3.967	−3.217	−1.787	−0.737	−1.6595	2.2559	0.4016	0.9990	[−2.15, 0.37]	3.70	–	–	–	−4.905	−3.651	−4.7826	3.0581	–	1	[−0.04, 0.37]
2.68	−4.719	−3.997	−3.244	−1.826	−0.786	−1.6989	2.2354	0.3924	0.9990	[−2.15, 0.37]	3.71	–	–	–	−4.919	−3.674	−4.7978	3.0367	–	1	[−0.04, 0.37]
2.69	−4.756	−4.028	−3.272	−1.864	−0.833	−1.7377	2.2156	0.3834	0.9990	[−2.15, 0.37]	3.72	–	–	–	−4.932	−3.697	−4.8118	3.0125	–	1	[−0.04, 0.37]
2.70	−4.793	−4.058	−3.299	−1.901	−0.880	−1.7758	2.1963	0.3746	0.9991	[−2.15, 0.37]	3.73	–	–	–	−4.944	−3.720	−4.8247	2.9852	–	1	[−0.04, 0.37]
2.71	−4.829	−4.088	−3.325	−1.938	−0.926	−1.8134	2.1776	0.3660	0.9991	[−2.15, 0.37]	3.74	–	–	–	−4.954	−3.743	−4.8363	2.9547	–	1	[−0.04, 0.37]
2.72	−4.865	−4.118	−3.351	−1.975	−0.971	−1.8504	2.1595	0.3577	0.9991	[−2.15, 0.37]	3.75	–	–	–	−4.963	−3.766	−4.8466	2.9209	–	1	[−0.04, 0.37]
2.73	−4.901	−4.148	−3.377	−2.011	−1.015	−1.8869	2.1420	0.3496	0.9992	[−2.15, 0.37]	3.76	–	–	–	−4.971	−3.789	−4.8555	2.8837	–	1	[−0.04, 0.37]
2.74	−4.936	−4.177	−3.403	−2.047	−1.058	−1.9229	2.1250	0.3417	0.9992	[−2.15, 0.37]	3.77	–	–	–	−4.977	−3.811	−4.8631	2.8429	–	1	[−0.04, 0.37]
2.75	−4.971	−4.206	−3.428	−2.083	−1.101	−1.9583	2.1085	0.3341	0.9992	[−2.15, 0.37]	3.78	–	–	–	−4.981	−3.834	−4.8691	2.7984	–	1	[−0.04, 0.37]
2.76	−5.005	−4.235	−3.453	−2.118	−1.142	−1.9933	2.0926	0.3267	0.9992	[−2.15, 0.37]	3.79	–	–	–	−4.984	−3.856	−4.8736	2.7500	–	1	[−0.04, 0.37]
2.77	−5.039	−4.264	−3.478	−2.153	−1.183	−2.0278	2.0772	0.3196	0.9993	[−2.15, 0.37]	3.80	–	–	–	−4.984	−3.878	−4.8765	2.6975	–	1	[−0.04, 0.37]

Note. The 11th and 22nd columns give the range of the metallicity [Fe/H] (dex) for the star whose absolute magnitude would be estimated. R^2 is the square of the correlation coefficient.

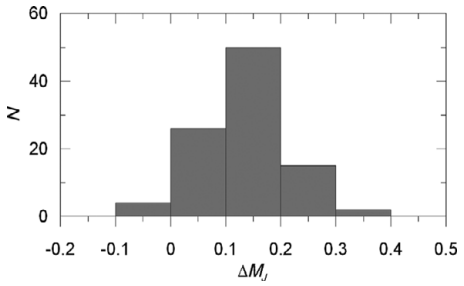

Figure 7. Histogram of the residuals for ΔM_J.

Table 14. Data for the Clusters Used for the Application of the Procedure

Cluster	$E(B-V)$ (mag)	μ_0 (mag)	[Fe/H] (dex)	Ref.
M5	0.038	14.330	−1.17	1, 2
M68	0.060	14.994	−2.01	3
NGC 188	0.087	11.130	−0.01	4, 5

References: (1) Brasseur et al. (2010); (2) Sandquist et al. (1996); (3) VandenBerg & Clem (2003); (4) Stetson, McClure, & VandenBerg (2004); (5) Meibom et al. (2009).

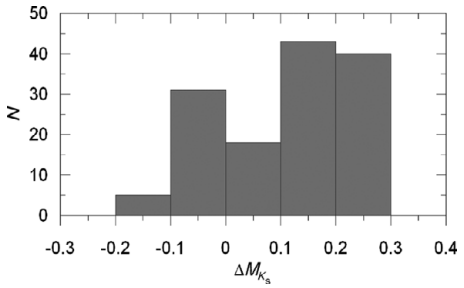

Figure 8. Histogram of the residuals for ΔM_{K_s}.

Table 15. $J_0 \times (V-J)_0$ Fiducial Giant Sequences for the Clusters M5 and M68 Used in the Application of the Procedure

Cluster	V	$V-J$	J	$(V-J)_0$	J_0
M5	12.31	2.59	9.72	2.505	9.687
	12.50	2.47	10.03	2.385	9.997
	12.68	2.36	10.32	2.275	10.287
	12.86	2.27	10.59	2.185	10.557
	13.09	2.18	10.91	2.095	10.877
	13.29	2.12	11.17	2.035	11.137
	13.49	2.06	11.43	1.975	11.397
	13.71	2.00	11.71	1.915	11.677
	13.91	1.95	11.96	1.865	11.927
	14.14	1.89	12.25	1.805	12.217
	14.35	1.84	12.51	1.755	12.477
	14.57	1.79	12.78	1.705	12.747
	14.80	1.74	13.06	1.655	13.027
	15.04	1.70	13.34	1.615	13.307
	15.27	1.67	13.60	1.585	13.567
	15.55	1.63	13.92	1.545	13.887
	15.81	1.60	14.21	1.515	14.177
	16.05	1.57	14.48	1.485	14.447
	16.33	1.54	14.79	1.455	14.757
	16.57	1.51	15.06	1.425	15.027
	16.83	1.50	15.33	1.415	15.297
	17.08	1.48	15.60	1.395	15.567
	17.32	1.47	15.85	1.385	15.817
	17.54	1.46	16.08	1.375	16.047
M68	1.234	1.196	12.497	2.203	10.294
	1.202	1.154	12.844	2.146	10.698
	1.047	0.951	13.498	1.868	11.630
	0.965	0.855	14.143	1.733	12.410
	0.905	0.775	14.744	1.624	13.120
	0.863	0.732	15.209	1.561	13.648
	0.803	0.669	15.775	1.471	14.304
	0.792	0.646	16.228	1.442	14.786
	0.752	0.626	16.645	1.405	15.240
	0.754	0.619	16.915	1.398	15.517
	0.739	0.609	17.215	1.382	15.833

reference refers to the colour excess and the distance modulus. The K_{s_0} magnitudes and $(V-K_s)_0$ colours as well as the original V, $B-V$, and $V-I$ data are given in Table 18.

We evaluated the M_{K_s} absolute magnitude by Equation (9) for a set of $(V-K_s)_0$ colour indices where the clusters are defined. The results are given in Table 19. The columns refer to (1) $(V-K_s)_0$ colour index; (2) $(M_{K_s})_{cl}$, the absolute magnitude for a cluster estimated by its colour–magnitude diagram; (3) $(M_{K_s})_{ev}$, the absolute magnitude estimated by the procedure; (4) ΔM_{K_s}, absolute magnitude residuals. Also, the metallicity for each cluster is indicated near the name of the cluster. The differences between the absolute magnitudes estimated by the procedure presented in this study and those evaluated via the colour–magnitude diagrams of the clusters (the residuals) lie in a short interval, i.e. −0.10 and +0.27 mag. The mean and the standard deviation of the residuals are $\langle \Delta M_{K_s} \rangle = 0.109$ and $\sigma_{M_{K_s}} = 0.123$ mag, respectively. The distribution of the residuals is given in Table 20 and Figure 8. The residuals for the cluster NGC 188 for the colour interval $2.15 \leq (V-K_s)_0 \leq 2.44$, where the metallicity of NGC 188 ([Fe/H] = −0.01 dex) fall off the metallicity interval corresponding to the cited colour interval, $-2.15 \leq$ [Fe/H] ≤ -0.04 dex, are slightly larger than those for $2.45 \leq (V-K_s)_0 \leq 2.60$ where the metallicity interval, $-2.15 \leq$ [Fe/H] $\leq +0.37$ dex, covers the metallicity of NGC 188. Although the larger residuals are given in Table 19, they are not considered in the statistics.

4 SUMMARY AND DISCUSSION

We calibrated the absolute magnitudes M_J and M_{K_s} for red giants in terms of metallicity by means of the colour–magnitude diagrams of the clusters M92, M13, M71, M67, and NGC 6791 with different metallicities. The $J \times (V-J)$ and $K_s \times (V-K_s)$ sequences used for the calibration of M_J and M_{K_s} are provided from different sources and by different procedures, as explained in the following. The main source is the paper of Brasseur et al. (2010). The

Table 16. $(M_J)_{ev}$ Absolute Magnitudes and ΔM_J Residuals Estimated by the Procedure Explained in Our Work. $(M_J)_{cl}$ Denotes the Absolute Magnitude Evaluated by Means of the Colour–Magnitude Diagram of the Cluster

$(V-J)_0$	$(M_J)_{cl}$	$(M_J)_{ev}$	ΔM_J	$(V-J)_0$	$(M_J)_{cl}$	$(M_J)_{ev}$	ΔM_J
	M5 ([Fe/H] = −1.17 dex)				M5 (cont.)		
1.40	1.203	0.876	0.327	2.38	−4.385	−4.417	0.033
1.42	0.928	0.630	0.298	2.40	−4.432	−4.475	0.043
1.44	0.670	0.410	0.260	2.42	−4.474	−4.532	0.058
1.46	0.428	0.198	0.230	2.44	−4.511	−4.588	0.077
1.48	0.200	−0.005	0.205	2.46	−4.540	−4.642	0.102
1.50	−0.013	−0.200	0.187	2.48	−4.562	−4.695	0.133
1.52	−0.214	−0.388	0.173	2.50	−4.577	−4.747	0.170
1.54	−0.403	−0.568	0.164		M68 ([Fe/H] = −2.01 dex)		
1.56	−0.581	−0.741	0.159	1.40	0.437	0.095	0.342
1.58	−0.749	−0.947	0.198	1.42	0.140	−0.146	0.286
1.60	−0.907	−1.099	0.192	1.44	−0.136	−0.373	0.236
1.62	−1.056	−1.245	0.188	1.46	−0.394	−0.588	0.195
1.64	−1.198	−1.385	0.188	1.48	−0.633	−0.792	0.159
1.66	−1.332	−1.520	0.189	1.50	−0.855	−0.986	0.131
1.68	−1.459	−1.650	0.191	1.52	−1.063	−1.170	0.108
1.70	−1.580	−1.775	0.195	1.54	−1.256	−1.346	0.090
1.72	−1.696	−1.920	0.224	1.56	−1.436	−1.513	0.077
1.74	−1.807	−2.027	0.220	1.58	−1.604	−1.690	0.086
1.76	−1.913	−2.131	0.217	1.60	−1.761	−1.839	0.078
1.78	−2.016	−2.231	0.215	1.62	−1.909	−1.982	0.073
1.80	−2.115	−2.329	0.214	1.64	−2.047	−2.119	0.071
1.82	−2.211	−2.423	0.212	1.66	−2.178	−2.250	0.072
1.84	−2.304	−2.514	0.210	1.68	−2.301	−2.376	0.075
1.86	−2.396	−2.603	0.207	1.70	−2.417	−2.498	0.081
1.88	−2.485	−2.689	0.204	1.72	−2.529	−2.614	0.086
1.90	−2.573	−2.773	0.200	1.74	−2.635	−2.728	0.094
1.92	−2.659	−2.854	0.195	1.76	−2.736	−2.839	0.103
1.94	−2.744	−2.933	0.189	1.78	−2.835	−2.946	0.112
1.96	−2.828	−3.010	0.181	1.80	−2.929	−3.051	0.121
1.98	−2.912	−3.085	0.173	1.82	−3.022	−3.153	0.131
2.00	−2.995	−3.158	0.163	1.84	−3.112	−3.251	0.140
2.02	−3.077	−3.229	0.152	1.86	−3.200	−3.348	0.148
2.04	−3.159	−3.298	0.139	1.88	−3.287	−3.442	0.156
2.06	−3.240	−3.365	0.125	1.90	−3.373	−3.535	0.162
2.08	−3.321	−3.431	0.110	1.92	−3.458	−3.625	0.167
2.10	−3.402	−3.496	0.094	1.94	−3.542	−3.714	0.172
2.12	−3.482	−3.559	0.077	1.96	−3.626	−3.800	0.174
2.14	−3.561	−3.620	0.059	1.98	−3.709	−3.885	0.176
2.16	−3.640	−3.680	0.040	2.00	−3.792	−3.968	0.176
2.18	−3.717	−3.739	0.021	2.02	−3.875	−4.049	0.174
2.20	−3.794	−3.796	0.002	2.04	−3.957	−4.127	0.170
2.22	−3.869	−3.887	0.018	2.06	−4.039	−4.205	0.165
2.24	−3.943	−3.907	−0.036	2.08	−4.121	−4.280	0.159
2.26	−4.014	−3.960	−0.054	2.10	−4.202	−4.352	0.150
2.28	−4.084	−4.012	−0.072	2.12	−4.281	−4.422	0.141
2.30	−4.151	−4.075	−0.076	2.14	−4.360	−4.489	0.129
2.32	−4.215	−4.237	0.022	2.16	−4.437	−4.554	0.117
2.34	−4.275	−4.298	0.023	2.18	−4.512	−4.616	0.103
2.36	−4.332	−4.358	0.026	2.20	−4.585	−4.673	0.088

$J \times (V-J)$ and $K_s \times (V-K_s)$ sequences for the clusters M92, M13, and M71 are taken from the tables of Brasseur et al. (2010), whereas the $J_0 \times (V-J)_0$ sequence for M67 and NGC 6791 is obtained by transformation of V, $B-V$, and $V-I$ data from Montgomery et al. (1993) and by means of the $M_V \times (V-J)_0$ diagram from Brasseur et al. (2010), respectively. Also, the $K_s \times (V-K_s)$ sequence for M67 is transformed from V, $B-V$, and $V-I$ data in Montgomery et al. (1993). The fiducial sequence for NGC 6791 is given in $K_s \times (J-K_s)$ in Brasseur et al. (2010). We

Table 17. Distribution of the Residuals. *N* Denotes the Number of Stars

ΔM_J Interval	$\langle \Delta M_J \rangle$	*N*
(−0.1, 0.0]	− 0.059	4
(0.0, 0.1]	0.060	26
(0.1, 0.2]	0.158	50
(0.2, 0.3]	0.229	15
(0.3, 0.4]	0.335	2

Table 18. $K_s \times (V-K_s)_0$ Fiducial Giant Sequences for the Clusters NGC 188 and M68 Used in the Application of the Procedure

Cluster	V_0	$(B-V)_0$	$(V-I)_0$	$(V-K_s)_0$	K_{s_0}
NGC 188	12.481	1.119	1.112	2.608	9.873
	13.031	1.052	1.063	2.474	10.557
	13.547	0.999	1.022	2.367	11.180
	14.069	0.954	0.991	2.277	11.792
	14.609	0.839	0.899	2.044	12.565
	14.786	0.819	0.885	2.004	12.782
M68	12.497	1.196	1.234	3.040	9.457
	12.844	1.154	1.202	2.955	9.889
	13.498	0.951	1.047	2.546	10.952
	14.143	0.855	0.965	2.350	11.793
	14.744	0.775	0.905	2.189	12.555
	15.209	0.732	0.863	2.100	13.109
	15.775	0.669	0.803	1.970	13.805
	16.228	0.646	0.792	1.925	14.303
	16.645	0.626	0.752	1.878	14.767
	16.915	0.619	0.754	1.866	15.049
	17.215	0.609	0.739	1.843	15.372

transformed the J_0 magnitudes to the V_0 ones obtained from the $M_V \times (V-J)_0$ diagram and altered the $K_s \times (J-K_s)$ data to $K_s \times (V-K_s)$ ones. Thus, we obtained two sets of data for two absolute magnitude calibrations, i.e. $J_0 \times (V-J)_0$ and $K_{s_0} \times (V-K_s)_0$ for M_J and M_{K_s}, respectively. We combined each set of data for each cluster with their true distance modulus and evaluated two sets of absolute magnitudes for the $(V-J)_0$ and $(V-K_s)_0$ ranges of each cluster. Then, we fitted M_J and M_{K_s} absolute magnitudes in terms of iron metallicity, [Fe/H], by quadratic polynomials, for a given $(V-J)_0$ and $(V-K_s)_0$ colour index, respectively. The calibrations cover large ranges, i.e. $1.30 \leq (V-J)_0 \leq 2.80$ and $1.75 \leq (V-K_s)_0 \leq 3.80$ mag for M_J and M_{K_s}, respectively.

We evaluated the M_J absolute magnitudes of the clusters M5 ([Fe/H] = −1.17 dex) and M68 ([Fe/H] = −2.01 dex) by the procedure presented in our study for a set of $(V-J)_0$ colour index and compared them with those estimated via combination of the fiducial $J_0 \times (V-J)_0$ sequence and the true distance modulus for each cluster. The total of the residuals lie between −0.08 and +0.34 mag, and the range of 94% of them is $0 < \Delta M_J \leq 0.3$ mag. The mean and the standard deviation of (all) the residuals are $\langle \Delta M_J \rangle = 0.137$ and $\sigma_{M_J} = 0.080$ mag. For the evaluation of the M_{K_s} absolute magnitudes, we applied the corresponding procedure to the clusters NGC 188 ([Fe/H] = −0.01 dex) and M68 ([Fe/H] = −2.01 dex). Here again, the range of the residuals, their mean and standard deviation are small, i.e. $-0.10 < \Delta M_{K_s} \leq +0.27$ mag, $\langle \Delta M_{K_s} \rangle = 0.109$, and $\sigma_{M_{K_s}} = 0.123$ mag.

We compared the statistical results obtained in this study with those of Papers I and II. Table 21 shows that M_V, M_g, M_J, and M_{K_s} absolute magnitudes can be estimated with an error less than 0.3 mag. However, one can notice an improvement on M_J and M_{K_s} with respect to M_V and M_g. The main difference between the data of the clusters in three studies is the large domain of the clusters in $(V-J)_0$ and $(V-K_s)_0$ which probably contributed to more accurate calibrations of the apparent J_0 and K_s magnitudes in terms of the corresponding colours with respect to $(B-V)_0$ and $(g-r)_0$ ones. Accurate calibration in apparent magnitude provided accurate absolute magnitudes. The magnitudes and colours for the cluster M67 used in the calibration of M_J and M_{K_s} absolute magnitudes are not original, but they are transformed from the $V, B-V$, and $V-I$ data by means of the equations of Yaz et al. (2010). The same case holds for the clusters NGC 188 and M68 which are used in the application of the procedure. Calibrations with high correlation coefficients and small residuals also confirm the equations of Yaz et al. (2010). As claimed in Papers I and II, there was an improvement in the results therein with respect to those of Hog & Flynn (1998). Hence, the same improvement holds for this study. We also quote the work of Ljunggren & Oja (1966).

Although age plays an important role in the trend of the fiducial sequence of the RGB, we have not used it as a parameter in the calibration of absolute magnitude. A quadratic calibration in terms of (only) metallicity provides absolute magnitudes with high accuracy. Another problem may originate from the red clump (RC) stars. These stars lie very close to the RGB but they present a completely different group of stars. Tables 16 and 19 and Figures 7 and 8 summarise how reliable are our absolute magnitudes. If age and possibly the mix with RC stars would affect our results, this should up. In addition, we should add that the fiducial sequences used in our study were properly selected as RGB. However, the researchers should identify and exclude the RC stars when they apply our calibrations to the field stars.

The accuracy of the estimated absolute magnitudes depends mainly on the accuracy of metallicity. We altered the metallicity by [Fe/H] + Δ[Fe/H] in evaluation of the absolute magnitudes by the procedure presented in our study and we checked its effect on the absolute magnitude. We adopted [Fe/H] = −2.01, −1.117, −0.01 dex and Δ[Fe/H] = 0.05, 0.10, 0.15, 0.20 dex and re-evaluated the absolute magnitudes for ten $(V-J)_0$ and nine $(V-K_s)$ colour indices for this purpose. The differences between the absolute magnitudes evaluated in this way and the corresponding ones evaluated without Δ[Fe/H] increments are given in Table 22. The maximum absolute magnitude differences corresponding to Δ[Fe/H] = 0.20 dex in M_J and M_{K_s}

Table 19. $(M_{K_s})_{ev}$ Absolute Magnitudes and ΔM_{K_s} Residuals Estimated by the Procedure Explained in Our Work. $(M_{K_s})_{cl}$ Denotes the Absolute Magnitude Evaluated by Means of the Colour–Magnitude Diagram of the Cluster

$(V-K_s)_0$	$(M_{K_s})_{cl}$	$(M_{K_s})_{ev}$	ΔM_{K_s}	$(V-K_s)_0$	$(M_{K_s})_{cl}$	$(M_{K_s})_{ev}$	ΔM_{K_s}	$(V-K_s)_0$	$(M_{K_s})_{cl}$	$(M_{K_s})_{ev}$	ΔM_{K_s}
NGC 188 ([Fe/H] = −0.01 dex)				M68 (cont.)				M68 (cont.)			
2.15	1.092	1.029	0.063	1.93	−0.671	−0.691	0.020	2.49	−3.735	−3.876	0.141
2.16	1.061	0.963	0.097	1.94	−0.765	−0.771	0.006	2.50	−3.768	−3.917	0.149
2.17	1.029	0.898	0.131	1.95	−0.857	−0.850	−0.007	2.51	−3.802	−3.958	0.156
2.18	0.996	0.832	0.163	1.96	−0.947	−0.928	−0.020	2.52	−3.835	−3.999	0.164
2.19	0.962	0.767	0.194	1.97	−1.035	−1.004	−0.031	2.53	−3.868	−4.039	0.171
2.20	0.926	0.702	0.224	1.98	−1.121	−1.079	−0.041	2.54	−3.902	−4.079	0.178
2.21	0.890	0.638	0.252	1.99	−1.204	−1.155	−0.050	2.55	−3.934	−4.120	0.185
2.22	0.852	0.574	0.278	2.00	−1.286	−1.227	−0.059	2.56	−3.967	−4.159	0.191
2.23	0.812	0.511	0.302	2.01	−1.365	−1.298	−0.067	2.57	−4.000	−4.197	0.198
2.24	0.771	0.447	0.324	2.02	−1.443	−1.369	−0.074	2.58	−4.032	−4.236	0.204
2.25	0.728	0.385	0.344	2.03	−1.518	−1.439	−0.080	2.59	−4.065	−4.275	0.210
2.26	0.684	0.322	0.361	2.04	−1.592	−1.508	−0.085	2.60	−4.097	−4.313	0.216
2.27	0.637	0.261	0.377	2.05	−1.664	−1.575	−0.089	2.61	−4.129	−4.351	0.221
2.28	0.589	0.199	0.390	2.06	−1.735	−1.642	−0.093	2.62	−4.162	−4.388	0.227
2.29	0.539	0.139	0.401	2.07	−1.803	−1.707	−0.096	2.63	−4.194	−4.426	0.232
2.30	0.488	0.078	0.409	2.08	−1.870	−1.772	−0.098	2.64	−4.226	−4.463	0.237
2.31	0.434	0.019	0.415	2.09	−1.936	−1.836	−0.100	2.65	−4.258	−4.499	0.241
2.32	0.379	−0.143	0.522	2.10	−2.000	−1.899	−0.101	2.66	−4.290	−4.535	0.246
2.33	0.322	−0.099	0.421	2.11	−2.062	−1.961	−0.102	2.67	−4.322	−4.571	0.250
2.34	0.264	−0.157	0.421	2.12	−2.124	−2.022	−0.101	2.68	−4.354	−4.607	0.253
2.35	0.204	−0.215	0.418	2.13	−2.183	−2.082	−0.101	2.69	−4.386	−4.642	0.256
2.36	0.142	−0.271	0.414	2.14	−2.242	−2.142	−0.099	2.70	−4.418	−4.677	0.259
2.37	0.080	−0.328	0.407	2.15	−2.299	−2.223	−0.076	2.71	−4.449	−4.712	0.262
2.38	0.016	−0.383	0.399	2.16	−2.355	−2.281	−0.074	2.72	−4.481	−4.746	0.265
2.39	−0.049	−0.439	0.389	2.17	−2.409	−2.338	−0.071	2.73	−4.513	−4.780	0.267
2.40	−0.115	−0.493	0.378	2.18	−2.463	−2.395	−0.068	2.74	−4.545	−4.814	0.269
2.41	−0.181	−0.547	0.366	2.19	−2.515	−2.451	−0.064	2.75	−4.577	−4.847	0.270
2.42	−0.248	−0.600	0.352	2.20	−2.566	−2.506	−0.060	2.76	−4.608	−4.880	0.271
2.43	−0.316	−0.653	0.337	2.21	−2.616	−2.560	−0.056	2.77	−4.640	−4.912	0.272
2.44	−0.383	−0.705	0.322	2.22	−2.665	−2.614	−0.051	2.78	−4.672	−4.944	0.272
2.45	−0.450	−0.634	0.184	2.23	−2.714	−2.668	−0.046	2.79	−4.704	−4.976	0.272
2.46	−0.517	−0.691	0.174	2.24	−2.761	−2.720	−0.041	2.80	−4.735	−5.007	0.272
2.47	−0.583	−0.747	0.163	2.25	−2.807	−2.772	−0.035	2.81	−4.767	−5.038	0.271
2.48	−0.649	−0.801	0.152	2.26	−2.853	−2.824	−0.029	2.82	−4.798	−5.068	0.270
2.49	−0.713	−0.855	0.142	2.27	−2.898	−2.875	−0.023	2.83	−4.830	−5.098	0.268
2.50	−0.775	−0.908	0.133	2.28	−2.941	−2.925	−0.016	2.84	−4.861	−5.127	0.266
2.51	−0.836	−0.960	0.124	2.29	−2.985	−2.975	−0.010	2.85	−4.893	−5.156	0.264
2.52	−0.894	−1.011	0.117	2.30	−3.027	−3.024	−0.003	2.86	−4.924	−5.185	0.261
2.53	−0.950	−1.061	0.111	2.31	−3.069	−3.073	0.004	2.87	−4.955	−5.213	0.258
2.54	−1.003	−1.111	0.107	2.32	−3.110	−3.224	0.114	2.88	−4.986	−5.241	0.255
2.55	−1.053	−1.159	0.106	2.33	−3.150	−3.169	0.019	2.89	−5.017	−5.268	0.251
2.56	−1.099	−1.207	0.108	2.34	−3.190	−3.217	0.026	2.90	−5.048	−5.294	0.247
2.57	−1.141	−1.254	0.113	2.35	−3.230	−3.264	0.034	2.91	−5.078	−5.321	0.242
2.58	−1.178	−1.300	0.122	2.36	−3.268	−3.310	0.042	2.92	−5.109	−5.346	0.237
2.59	−1.210	−1.345	0.135	2.37	−3.307	−3.356	0.050	2.93	−5.139	−5.370	0.231
2.60	−1.237	−1.390	0.153	2.38	−3.344	−3.402	0.057	2.94	−5.169	−5.395	0.225
M68 ([Fe/H] = −2.01 dex)				2.39	−3.382	−3.447	0.065	2.95	−5.199	−5.418	0.219
1.84	0.295	0.096	0.199	2.40	−3.419	−3.492	0.073	2.96	−5.229	−5.441	0.212
1.85	0.177	0.002	0.175	2.41	−3.455	−3.536	0.081	2.97	−5.259	−5.464	0.205
1.86	0.061	−0.090	0.151	2.42	−3.491	−3.580	0.089	2.98	−5.288	−5.486	0.198
1.87	−0.051	−0.180	0.129	2.43	−3.527	−3.624	0.097	2.99	−5.317	−5.507	0.190
1.88	−0.161	−0.269	0.108	2.44	−3.562	−3.667	0.105	3.00	−5.346	−5.527	0.181
1.89	−0.268	−0.356	0.088	2.45	−3.597	−3.707	0.110	3.01	−5.374	−5.547	0.173
1.90	−0.372	−0.442	0.069	2.46	−3.632	−3.750	0.118	3.02	−5.402	−5.566	0.164
1.91	−0.474	−0.526	0.052	2.47	−3.666	−3.792	0.126	3.03	−5.430	−5.583	0.154
1.92	−0.574	−0.609	0.035	2.48	−3.701	−3.834	0.133	3.04	−5.457	−5.601	0.144

Table 20. Distribution of the Residuals. *N* Denotes the Number of Stars

ΔM_{K_s} Interval	$\langle \Delta M_{K_s} \rangle$	N
(−0.2, −0.1]	−0.101	5
(−0.1, 0.0]	−0.055	31
(0.0, 0.1]	0.050	18
(0.1, 0.2]	0.148	43
(0.2, 0.3]	0.248	40

Table 21. Comparison of the Results in Three Studies. The Word "all" Indicates all the Residuals. A Subset of the Residuals Is Denoted by a Percentage, Such as 91% or 94%

ΔM Range	$\langle \Delta M \rangle$	σ	Study
(−0.61, +0.66) (all) [−0.40, 0.40] (91%)	0.05 (91%)	0.190 (91%)	Paper I
(−0.28, +0.43] (all) (0.10, 0.40], (94%)	0.169 (all)	0.140 (all)	Paper II
(−0.08, +0.34] (all) (0.00, 0.30] 94%	0.137 (all)	0.080 (all)	This study, ΔM_J
(−0.10, +0.27]	0.109	0.123	This study, ΔM_{K_s}

lie in the intervals $0.09 \leq \Delta M_J \leq 0.31$ and $0.05 \leq \Delta M_{K_s} \leq 0.14$, respectively, for the metallicities [Fe/H] = −1.117 and [Fe/H] = −2.01 dex. However, they are about 0.5 mag for the metallicity [Fe/H] = −0.01 dex. The mean error in metallicity for 42 globular and 33 open clusters in the catalogue of Santos & Piatti (2004) is $\sigma = 0.19$ dex. If we assume the same error for the field stars, the probable error in M_J and M_{K_s} would be less than 0.3 mag for relatively metal-poor stars. However, for the solar metallicity stars, the metallicity error should be $\sigma_{[Fe/H]} < 0.15$ dex in order to estimate accurate absolute magnitudes. That is, the solar metallicities should be determined more preciously.

The absolute magnitudes can be calibrated as a function of ultraviolet excess instead of metallicity, in general. However, an ultraviolet band is not defined in 2MASS photometry. Hence, we calibrated the M_J and M_{K_s} absolute magnitudes in terms of metallicity which can be determined by means of atmospheric model parameters. Age is a secondary parameter for the old clusters and does not influence much the position of their RGB. The youngest cluster in our study is M67 with an age of 4 Gyr (Paper I). However, the field stars may be younger. Recall that the derived relations are applicable to stars older than 4 Gyr.

We conclude that the two absolute magnitudes, M_J and M_{K_s}, in 2MASS photometry can be estimated for the red giants in terms of metallicity with an accuracy of $\Delta M \leq 0.3$ mag. Our target in the near future would be to adopt this procedure to RC stars.

Table 22. Absolute Magnitudes Estimated by Altering the Metallicity as [Fe/H] + Δ[Fe/H]

	M_J					ΔM_J				
$(V-J)_0$	(1)	(2)	(3)	(4)	(5)	(6)	(7)	(8)	(9)	
1.50	−0.200	−0.139	−0.076	−0.012	0.055	0.061	0.124	0.189	0.255	
1.70	−1.775	−1.703	−1.629	−1.550	−1.469	0.072	0.147	0.225	0.306	
1.90	−2.773	−2.707	−2.639	−2.568	−2.496	0.066	0.134	0.204	0.277	[Fe/H] = −1.117 + Δ[Fe/H]
2.10	−3.496	−3.431	−3.365	−3.298	−3.229	0.064	0.130	0.198	0.267	
2.30	−4.075	−4.007	−3.938	−3.868	−3.798	0.068	0.137	0.207	0.277	
2.50	−4.747	−4.707	−4.664	−4.619	−4.570	0.040	0.082	0.128	0.177	
1.50	−0.986	−0.952	−0.917	−0.879	−0.841	0.034	0.070	0.107	0.146	
1.70	−2.498	−2.481	−2.460	−2.436	−2.408	0.018	0.038	0.062	0.090	[Fe/H] = −2.01 + Δ[Fe/H]
1.90	−3.535	−3.508	−3.478	−3.446	−3.412	0.027	0.057	0.088	0.123	
2.10	−4.352	−4.313	−4.272	−4.230	−4.187	0.039	0.079	0.121	0.165	
	M_{K_s}					ΔM_{K_s}				
$(V-K_s)_0$	(1)	(2)	(3)	(4)	(5)	(6)	(7)	(8)	(9)	
2.45	−0.634	−0.489	−0.341	−0.190	−0.035	0.145	0.293	0.445	0.599	
2.50	−0.908	−0.772	−0.633	−0.491	−0.346	0.136	0.275	0.417	0.562	[Fe/H] = −0.01 + Δ[Fe/H]
2.55	−1.159	−1.031	−0.900	−0.766	−0.630	0.128	0.259	0.393	0.529	
2.60	−1.390	−1.268	−1.144	−1.018	−0.889	0.122	0.245	0.372	0.500	
1.85	0.002	0.024	0.048	0.074	0.103	0.022	0.046	0.072	0.101	
2.05	−1.575	−1.557	−1.536	−1.513	−1.487	0.018	0.039	0.063	0.089	
2.25	−2.772	−2.764	−2.753	−2.738	−2.719	0.008	0.019	0.034	0.053	[Fe/H] = −2.01 + Δ[Fe/H]
2.45	−3.707	−3.695	−3.679	−3.661	−3.639	0.012	0.027	0.046	0.068	
2.65	−4.499	−4.468	−4.434	−4.398	−4.361	0.031	0.065	0.101	0.138	

Notes. The numerical values of [Fe/H] are indicated in the last column. The absolute magnitudes in column (1) are the original ones taken from Tables 16 and 19, whereas those in columns (2)–(5) correspond to the increments 0.05, 0.10, 0.15, and 0.20 dex. The differences between the original absolute magnitudes and those evaluated by means of the increments are given in columns (6)–(9).

ACKNOWLEDGMENTS

This research has made use of NASA's Astrophysics Data System and the SIMBAD database, operated at CDS, Strasbourg, France

REFERENCES

Anthony-Twarog, B. J., Twarog, B. A., & Mayer, L. 2007, AJ, 133, 1585
Bilir, S., Karaali, S., Ak, S., Coşkunoğlu, K. B., Yaz, E., & Cabrera-Lavers, A. 2009, MNRAS, 396, 1589
Bilir, S., Karaali, S., Ak, S., Yaz, E., Cabrera-Lavers, A., & Coşkunoğlu, K. B. 2008, MNRAS, 390, 1569
Bilir, S., Karaali, S., Dağtekin, N. D., Önal, Ö., Ak, S., Ak, T., & Cabrera-Lavers, A. 2012, PASA, 29, 121
Brasseur, C. M., Stetson, P. B., VandenBerg, D. A., Casagrande, L., Bono, G., & Dall'Ora, M. 2010, AJ, 140, 1672
Breddels, M. A., et al. 2010, A&A, 511A, 90
Chen, B., et al. 2001, ApJ, 553, 184
ESA 1997, The Hipparcos and Tycho Catalogues (ESA SP-1200; Noordwijk: ESA)
Fiorucci, M., & Munari, U. 2003, A&A, 401, 781
Gratton, R. G. Fusi Pecci, F., Carretta, E., Clementini, G., Corsi, C. E., & Lattanzi, M. 1997, ApJ, 491, 749
Harris, W. E. 2010, arXiv1012.3224
Hodder, P. J. C., Nemec, J. M., Richer, H. B., & Fahlman, G. G. 1992, AJ, 103, 460
Hog, E., & Flynn, C. 1998, MNRAS, 294, 28
Karaali, S., Bilir, S., & Yaz Gökçe, E. 2012a, PASA, 29, 509
Karaali, S., Bilir, S., & Yaz Gökçe, E. 2012b, PASA, in press (arXiv:1206.2752K) (Paper II)
Karaali, S., Karataş, Y., Bilir, S., Ak, S. G., & Hamzaoğlu, E. 2003, PASA, 20, 270
Laird, J. B., Carney, B. W., & Latham, D. W. 1988, AJ, 96, 1908
Ljunggren, B., & Oja, T. 1966, IAUS, 24, 317
McCall, M. L. 2004, AJ, 128, 2144
Meibom, S., et al. 2009, AJ, 137, 5086
Montgomery, K. A., Marschall, L. A., & Janes, K. A. 1993, AJ, 106, 181
Nissen, P. E., & Schuster, W. J. 1991, A&A, 251, 457
Phleps, S., Meisenheimer, K., Fuchs, B., & Wolf, C. 2000, A&A, 356, 108
Rosenberg, A., Saviane, I., Piotto, G., & Aparicio, A. 1999, AJ, 118, 2306
Sandquist, E. L., Bolte, M., Stetson, P. B., & Hesser, J. E. 1996, ApJ, 470, 910
Santos, J. F. C. Jr, & Piatti, A. E. 2004, A&A, 428, 79
Sandage, A., Lubin, L.M., & VandenBerg, D.A. 2003, PASP, 115, 1187
Sarajedini, A., Dotter, A., & Kirkpatrick, A. 2009, ApJ, 698, 1872
Savage, B. D., & Mathis, J. S. 1979, ARA&A, 17, 73
Saviane, I., Piotto, G., Fagotto, F., Zaggia, S., Capaccioli, M., & Aparicio, A. 1998, A&A, 333, 479
Siebert A., et al. 2011, AJ, 141, 187
Siegel, M. H., Majewski, S. R., Reid, I. N., & Thompson, I. B. 2002, ApJ, 578, 151
Skrutskie, M. F., et al. 2006, AJ, 131, 1163
Smith, R. G. 1987, MNRAS, 227, 943
Stetson, P. B., McClure, R. D., & VandenBerg, D. 2004, PASP, 116, 1012
Turner, D. G. 2011, RMxAA, 47, 127
Turner, D. G. 2012, Ap&SS, 337, 303
van Leeuwen, F. 2007, A&A, 474, 653
VandenBerg, D. A., & Clem, J. L. 2003, AJ, 126, 778
Walker, A. R. 1994, AJ, 108, 555
Yaz, E., Bilir, S., Karaali, S., Ak, S., Coşkunoğlu, B., & Cabrera-Lavers, A. 2010, AN, 331, 807
Zwitter, T., et al. 2010, A&A, 522A, 54